REVIEW   **Open Access**

Utilization of Solid Waste in the Production of Autoclaved Aerated Concrete and Their Effects on its Physio-mechanical and Microstructural Properties: Alternative Sources, Characterization, and Performance Insights

Abhilasha[1,2], Rajesh Kumar[1,2*] , Rajni Lakhani[1,2], Raghav Kumar Mishra[2] and Shahnavaz Khan[2]

Abstract

Autoclaved aerated concrete (AAC) is the lightest masonry material available in today's building industry. It shows properties, such as high strength per unit weight, lesser density, lower shrinkage, higher thermal insulation, and fire resistance as compared to traditional concrete. Not only engineering properties of AAC make it popular in construction industry, but also its eco-friendly nature also contributes in conservation of energy. AAC produces about 67% lower carbon emission than the clay bricks. Consequently, it becomes a cost-effective product which reduces the cost of construction. This paper provides thorough insight into possible solutions for the waste utilization. It has been inferred that fine aggregates can be replaced by these wastes in the preparation of AAC. This replacement will improve its physio-mechanical properties, such as bulk-density, moisture absorption, compressive strength, along with microstructure. These properties are comprehensively presented to categorize the investigation which has been done in such fields earlier. The ongoing research work at the author's institute, i.e., the development of lightweight concrete by using different kind of waste materials, such as marble slurry, fly ash, etc., is being presented.

Highlights

- The paper presents the feasibility to use different agro-industrial wastes to develop AAC.
- Studies on the effect of fiber reinforcement on the physio-mechanical properties of AAC have been discussed.
- Ca/Si ratio affects the tobermorite formation and the mineralogy of AAC.
- Influence of porosity on the microstructure of AAC has been investigated.
- Ongoing R&D work at the author's institute has been described.

Graphical Abstract

1 Introduction

Autoclaved aerated concrete (AAC) was invented in 1923, and extensively used worldwide. The estimated yearly worldwide production of AAC (non-reinforced) in recent years sums up to 450 million m^3 (Fouad & Schoch, 2018). It holds 16% of total construction in India; whereas, in the UK and Germany it contributes over 40 and 60% of total construction (Subash et al., 2016). AAC is assessed as lightweight building material with higher thermal resistivity and lower heat conduction. The density and compressive strength of AAC vary widely ranging from 451 to 1000 kg/m^3 and 1.5 to 7.0 MPa, respectively, as per IS: 2185 (Part 3). Its thermal insulation property reduces about 50% consumption of building energy (Rahman et al., 2020). Even there is no additional thermal insulating layers to the building walls in comparison of traditional concrete, hence maximize energy efficiency in buildings. Consequently, AAC counts as an environment friendly or green material (Rahman et al., 2020). AAC block generated around 67% less carbon emissions than clay brick (Yaman & Abd Rashid, 2021). Instead of using standard burnt clay brick, AAC block considerably lessened the environmental effect (Yaman & Abd Rashid, 2021).

Aerated concrete can be categorized as autoclaved aerated concrete (AAC) or non-autoclaved aerated concrete (NAAC) based on pore growth mechanism, cementitious materials used, and most importantly, the curing method (Narayanan & Ramamurthy, 2000). NAAC is a foamed concrete in which foaming agents are generally based on proteins, synthetic, and glue resins, etc. The AAC can be produced by two methods, chemical and mechanical

processes. The reaction of aluminum and calcium hydroxide generates hydrogen gas which is responsible for the porous shape with low weight (Rahman et al., 2020; Cai et al., 2019). Metallic compounds can also be used as an air-entraining agent in the chemical process for generating air bubbles within the concrete. However, in the mechanical process a variety of foaming agents can be used (Karakurt et al., 2010).

In general, AAC can be prepared under the condition of high pressure and temperature which should lie between 180 and 200 °C in a high-pressure autoclave (Narayanan & Ramamurthy, 2000). Generally, the production of AAC is carried by a homogeneous mixing of commonly available basic raw materials, such as mixture of quartz sand which should be ground finely, cement, lime and limiting quantity of aluminum powder (air-entraining agent). Air-entraining agent form pores when steam cured at high pressure and temperature (Kunchariyakun et al., 2015). During the process of autoclaving, AAC is strengthened due to the formation of the 1.1 nm calcium-silicate-hydrate (Ca$_5$Si$_6$O$_{16}$(OH)$_2$·4H$_2$O) in crystalline phase called Tobermorite in the fresh state as well as in hardened state (Qu & Zhao, 2017).

As the population and urbanization are increasing day by day, the consumption of natural resources for making building materials increasing simultaneously. Consequently, there is a massive increase in the generation of unmanaged waste in various industries. This continuous increment in unmanaged waste is the reason why many countries including India are facing serious environmental issues. Therefore, re-cyclization and consumption of waste for developing sustainable construction materials,

Abhilasha *et al. Int J Concr Struct Mater*   (2023) 17:6

Page 3 of 22

such as AAC is the need of today's world as well as it's an effective solution for managing the waste (Munir et al., 2018). Fig. 1 shows the recent observed country-wise and year-wise research pattern in the area of lightweight concrete (Source: https://www.scopus.com/, Keyword: Lightweight Concrete, Accessed on: 25–08–2022). These observations indicate the urgent need of attention in this research area.

1.1 Waste Substitution in AAC

Various studies have been conducted by combining different waste products [such as—rice husk ash (RHA), coal gangue, stone waste, solid municipal waste, etc.] into this course of action. RHA affects various parameters of AAC, such as physio-mechanical and microstructural

properties. AAC has been developed using different percentage of RHA at a temperature of 180 °C for 8 h. and 18 h. Microfine RHA particles showed positive effect as C-S-H transformed to tobermorite during the cement hydration (Kunchariyakun et al., 2015). Clinoptilolite which is known as natural zeolite, worked as an aggregate as well as a bubble-forming agent in the preparation of AAC. Physio-mechanical properties of AAC incorporated with clinoptilolite enhanced due to its coarser size of grain (Karakurt et al., 2010). Incorporation of sugar sediment waste as a raw material in the preparation of AAC improves the compressive strength which is the consequence of tobermorite formation in higher amount (Thongtha et al., 2014).
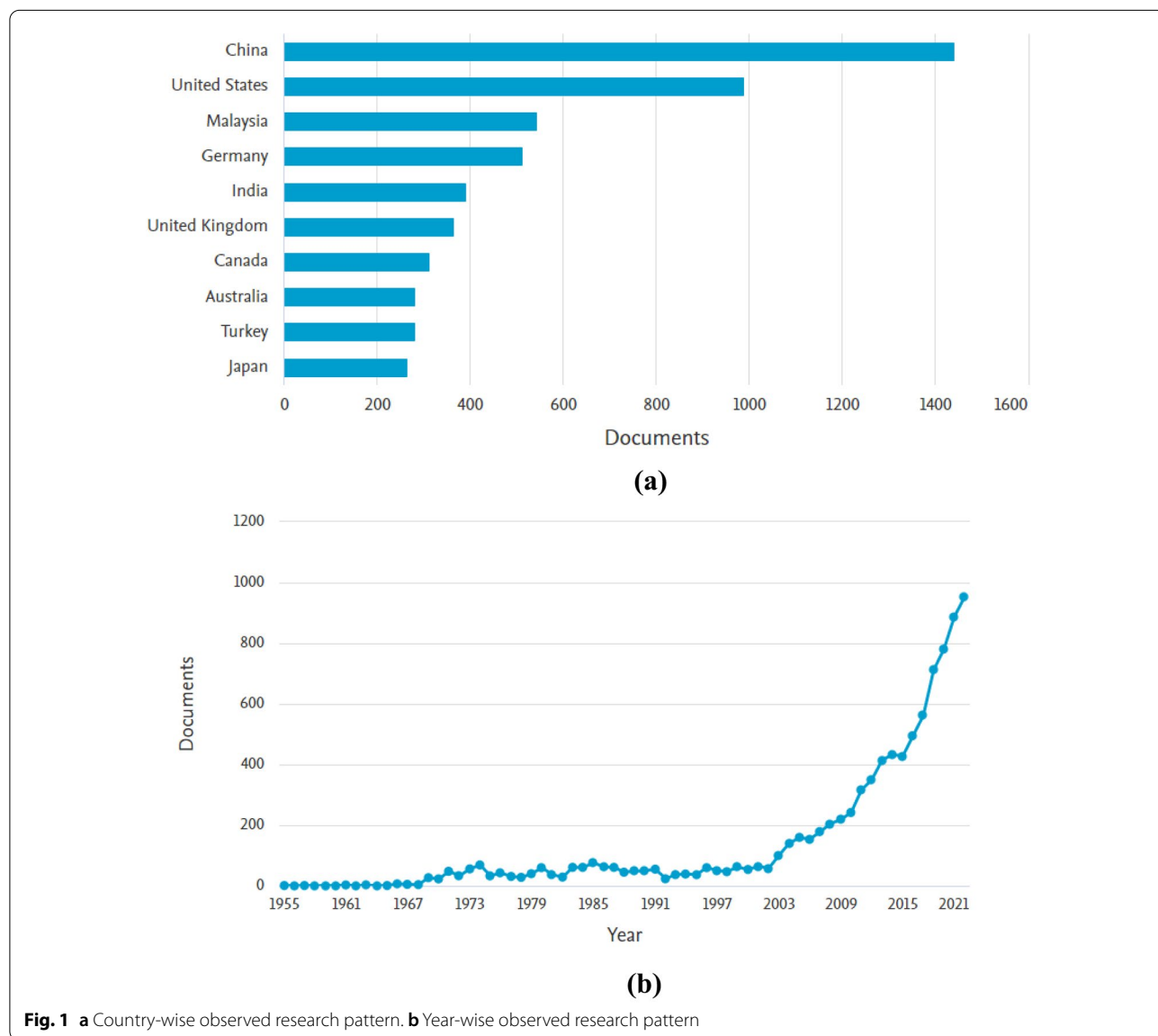

Fig. 1 a Country-wise observed research pattern. **b** Year-wise observed research pattern

In order to reduce the generation of iron ore tailings (IOTs) which is a waste produced from the steel industry, a new technology has been applied in which coal gangue (CG) is also used with IOTs as a siliceous material to develop AAC (Wang et al., 2016). AAC mix contains maximum percentages of siliceous compounds compared to other aggregates. Mineral-based aggregates, such as broken rock and granites are the major sources of silica which is the best alternative source of natural river sand (Zafar et al., 2020). Various properties of AAC, such as thermal, mechanical, and durability has been examined in several studies. The solid waste generated during the process of cutting, grinding or other processing of stone is known as stone sawing mud (SSM). Basically, it is a stone powder which contains lots of water (Alyamaç & Aydin, 2015). Quartz with soda feldspar and potassium feldspar are the major mineral composition of the stone sawing mud. So, the utilization of SSM is a problem subjected to the protection of the groundwater and environment. AAC formed with SSM have good thermal insulation performance (Wan et al., 2018).

To utilize the waste generated from the stone processing plant, stone dust is being used as a partial replacement of natural or quartz sand in AAC (Zafar et al., 2020). As a result, reduction in environmental and health hazards, takes place along with the control over excavation of river. This research was based on the feasible potential addition of the granite waste in the preparation of AAC. It has been found that granite waste effectively modifies the various properties in terms of physiomechanical, thermal and microstructural (Zafar et al., 2020). The final properties of AAC depend on the variation of several factors, such as quality of raw materials, mix design proportioning method, autoclaving time and temperature. Although a large number of research have been published, there is still much scope for improvement in optimizing composition, thermal performance, shrinkage, and long-term durability (Qu & Zhao, 2017). The manufacturing of AAC concrete using various types of wastes is shown in Table 1. This state of art is primarily focused on the utilization of different wastes in the preparation of AAC (Fig. 2).

1.2 Chemical Compositions of Waste Materials

Characterization of waste materials provides useful information about the nature of waste. Chemical compositions help in the selection of feasible solution by which that particular waste can be utilize effectively. Geographical locations are the prime factor for the compositions of waste. Same type of waste can show different properties if they have collected from different places. Still, we can conclude useful facts by the characterization, which will help for the further assessment. Chemical composition of various wastes is summarized in Table 2.

Wastes such as rice husk (Kunchariyakun et al., 2015), Zeolite Socony Mobil-5 (ZSM-5) (Jiang et al., 2021), black rice husk ash (BRHA) (Kunchariyakun et al., 2018), quartz tailing (Jin et al., 2016), and quartzite (Albayrak et al., 2007) are rich in silica content (90–95%). Due to the higher percentages of silica and alumina oxides $(SiO_2 + Al_2O_3 + Fe_2O_3 > 90\%)$, they are highly pozzolanic and active in nature; whereas wastes such as natural zeolite (Karakurt et al., 2010), sugar sediment (Thongtha et al., 2014), iron ore tailing (Wang et al., 2016), stone sawing mud (Wan et al., 2018), granite dust (Zafar et al., 2020), bagasse ash (Kunchariyakun et al., 2018), and glass cullet traces (Walczak et al., 2015a) contain 65–78% of silica content and can easily replace the quartz sand during the preparation of AAC. Traces of other chemicals, such as CaO, Fe_2O_3, K_2O, and MgO are also present in very less quantities.

2 Constituents of AAC

AAC consists of basic components, such as binders (cement, lime), fine aggregate (silica sand), gypsum, an air-entraining agent, and water. All the aforementioned ingredients will be discussed in detail in the following subsections.

2.1 Binder

In AAC, different calcareous and siliceous materials can be used as a binder (Narayanan & Ramamurthy, 2000). However, cement is the main component used for binding it. Generally, OPC and PPC are the types of cement that have been used (Hamad, 2014). However, lime as a calcareous material can replaced cement to some extent with percentages of cement up to 5% to increase the pozzolanic properties (Zafar et al., 2020). On the other hand, the raw siliceous material which is used in higher amounts in the preparation of AAC is quartz which is taken from natural resources. There are numerous studies in which natural sand has been replaced by waste material which enhanced the properties of AAC. This also helped to manage the industrial wastes, such as pulverized fuel ash, slate waste, and fly ash used to replace the binder or sand (Narayanan & Ramamurthy, 2000). Besides, silica fumes are beneficial for strength increment and affect thermal conductivity due to their higher pozzolanic properties (Qu & Zhao, 2017).

2.2 Micro-particles

Various types of pozzolanic additives in finely dispersed form are widely used to enhance the properties of concrete. Pozzolanic material can be natural or technogenic material having pozzolanic properties

Abhilasha *et al. Int J Concr Struct Mater*   (2023) 17:6

Page 5 of 22

Table 1 Preparation of AAC using various wastes

Waste	Characterization and uses	Observations	Refs.
Rice husk ash	Silica content is about 92.80%, therefore it can easily replace quartz sand during the formation of AAC	50% optimize replacement of sand has been done. Due to the higher reactivity, it decreased the autoclaving time by converting C-S-H into tobermorite efficiently	Kunchariyakun et. al. (2015)
Clinoptilolite (natural zeolite)	Rich in silica content (>75%) due to which it can work as an aggregate by replacing silica sand in AAC. Its calcined form can be used for generating bubbles in AAC due to the high surface energy after calcination	At 50% of optimum replacement of sand, compressive strength was increased by 27.9% whereas thermal conductance and unit weight (930 kg/m^3) was decreased by 11.6% and 14%, respectively. With calcined zeolite, compressive strength was observed as 4.6 MPa without using Al powder	Karakurt et. al. (2010)
Sugar sediments	It has almost similar chemical composition to that of sand (69.20% SiO_2). Therefore, it can be used as an alternative source of sand. Due to the presence of 15.57% CaO, it can be added as alternative to lime	7.5% and 30% replacement of sand and lime by weight has been done, respectively. As a results, higher compressive strength (6.1 MPa) and lower thermal conductivity (comparatively 26.3% less) was observed	Thongtha et. al. (2014)
Iron ore tailings (IOTs) and coal gangue (CG)	Around 68% and 34% silica content were presented in IOTs and CG, respectively	Combination of IOTs and CG replaced sand completely in AAC samples of 600 kg/m^3 density for which compressive strength was observed 3.68 MPa	Wang et. al. (2016)
Stone processing Mud (SPM)	Besides, 70% of SiO_2 and 15% of Al_2O_3, 3.5 and 4.5% K_2O and Na_2O presented, respectively	On 100% replacement of river sand, compressive strength was increased by 3.4% and porosity decreased by 1.3% (average pore size of 0.82 mm)	Wan et. al. (2018)
Granite dust	65% SiO_2 (average grain size of 15 μm) was presented with 15% of Fe_2O_3. Therefore, it can be used as an alternative source of silica rich fine aggregate for the preparation of AAC	At 20% optimal replacement, compressive strength was increased by 42%. With 5% solution of sulphuric acid (H_2SO_4) and hydrochloric acid (HCl), 32% and 54% higher acid resistance has been observed, respectively, when compared to control mix	Zafar et. al. (2020)
Solid municipal waste (incinerated bottom ash)	Contains 32% SiO_2, 29% CaO and 8.6% Al_2O_3. Works as a replacement of silica rich fine aggregate and aluminum powder	Improved strength with uniformity in pore structure. Decreased drying shrinkage	Song et. al. (2015)

Fig. 2 Different wastes used for AAC formation (Source: Google Images)

contains majorly active silica (SiO_2) (Laukaitis et al., 2010). This reacts with Portlandite constituent ($Ca(OH)_2$) in cementitious ingredients. This forms calcium-silicate-hydrate (C-S-H), as a result of additional strength in cementitious materials (Jo et al., 2007; Taylor, 1997). Sinica et. al. (2014) has investigated the performance of AAC which contains continuous basalt fibers (BF) and silica micro-dust (SMD), within recurrent cooling and heating cycles. It was confirmed that BF having 0.1–6 mm length, 4.6 μm an average diameter and SiO_2 micro-dust with about 20 μm average size particle, significantly enhanced the AAC stability (Sinica et al., 2014). After 25 cycles of cooling and heating, the compressive strength increases from 20 to 52%, bending strength increases from 27 to 62% and shrinkage deformation decreased by 25% when compared to normal samples without additives (Sinica et al., 2014).

Incorporation of nano-sized amorphous silica (AS) and carbon fiber (CF) in the formation of AAC, affects the properties of AAC forming mixture. At 1.0% of optimum replacement of sand by AS in the AAC mix, expansion of the forming mixture of AAC was increased by 11.0%. Temperature of the forming mix increased by 2.1%, compressive strength increased by 271.4%, and, ultrasonic impulse velocity (UIV) also

increased by 3.0% (Lekūnaitė et al., 2012); whereas, the optimal substitution of CF with sand by 0.1% decreased the temperature of forming mixture up to 1.5%, increased in volume up to 16.0% and increased in UIV up to 2.0% and increased plasticity strength up to 152.9% (Lekūnaitė et al., 2012).

2.3 Air-Entraining Agent
Aluminum is one of the most commonly used air-entraining agent in the preparation of AAC (Kalpana & Mohith, 2020). The intrusion of air in AAC is generally done by the addition of aluminum powder (AP), having very fine grain size. The aluminum powder reacts with the solvable bases presents in the cement/lime slurry to produce small sizes of bubbles (Narayanan & Ramamurthy, 2000). However, some municipal solid waste (MSW), such as incineration bottom ash (IBA) can be a substitute for the conventional AP. It can be used as an air-entraining agent in the formation of AAC. Fig. 3 represents the grain size distribution curves of three IBAs and AP (Song et al., 2015).

2.4 Fiber Addition
AAC is brittle in nature and having similarities to fiber-reinforced aerated concrete (FRAC) (Laukaitis et al., 2009). FRAC is lightweight AAC in which reinforcement has been done internally by using polymeric fibers (Laukaitis et al., 2009; Zollo, 1997). The micro-structures of AAC and FRAC show different textures. AAC having brittle behavior and under flexural or tensile loading, does not show any crack resistance nature. On the contrary, FRAC is a tough concrete and sufficiently dissipates large energy, because fiber prevents the opening of cracks by bridging action (Pehlivanlı et al., 2015). FRAC has significantly lower values of compressive strength than AAC, because room temperature curing is performed for the preparation of FRAC. Autoclaving process can damage polypropylene fibers and to prevent this damage, autoclaving process has been eliminated. This elimination of the autoclaving process in FRAC will result in a lower strength value and a higher degree of unevenness. FRAC had nearly half compressive strength than that of AAC samples but flexural strength of FRAC was 100 times greater than that of AAC. This was due to the presence of fibers, which act as a bridge between the macro- and micro-cracks (Laukaitis et al., 2009). However, fibers can increase the ductile properties of AAC by providing the bridging between micro- and macro-cracks (Laukaitis et al., 2009; Pehlivanlı et al., 2015).

Different fibers, such as polypropene, basalt, non-hydrophilic and hydrophilic carbon, and kaolin have

Abhilasha *et al. Int J Concr Struct Mater*   (2023) 17:6

Page 7 of 22

Table 2 Chemical composition of various wastes used in the formation of AAC

Waste materials	SiO_2	Al_2O_3	CaO	Fe_2O_3	FeO	Fe_2O	P_2O_5	SO_2	MgO	Na_2O	K_2O	$CaSO_4$	SO_3	LOI	Refs.
Rice husk	92.80	0.15	0.70	0.17	–	–	1.87	–	0.77	0.08	3.35	–	–	–	Kunchariyakun et. al. (2015)
Natural zeolite	77.07	13.56	2.36	1.59	–	–	–	–	1.45	0.11	3.86	–	–	–	Karakurt et. al. (2010)
Sugar sediment	69.20	7.08	15.57	0.92	–	–	–	–	0.12	0.90	1.20	–	–	–	Thongtha et. al. (2014)
Iron ore tailing	68.96	7.68	4.35	2.32	4.47	–	–	0.02	3.64	1.41	1.85	–	–	2.49	Wang et. al. (2016)
Coal gangue	34.05	26.00	0.67	0.49	1.70	–	–	0.28	0.61	–	0.16	–	–	32.76	
Autoclaved coal	51.05	36.71	1.05	3.12	0.42	–	–	–	0.92	–	0.23	–	–	0.72	
Stone sawing mud	72.66	15.09	1.56	1.15	–	–	–	–	0.38	4.54	3.58	–	–	0.42	Wan et. al. (2018)
Granite dust	65.53	5.39	9.50	15.09	–	–	–	–	–	–	2.60	–	–	1.89	Zafar et. al. (2020)
IBA	32.75	8.57	29.06	10.02	–	–	4.77	–	1.75	2.87	1.24	–	3.01	6.60	Song et. al. (2015)
EPS	70	14	3	2.4	–	–	–	–	0.2	7.6	–	–	–	1.7	Bonakdar et. al. (2013)
Lime sulphate ash	0.42	0.26	43.9	–	–	–	–	–	–	2.34	–	31.0	–	–	Hauser et. al. (1999)
Al-bearing ash	14.51	9.30	24.4	–	–	–	–	–	–	0.44	–	10.7	–	–	
Iron tailings	42.90	10.75	12.97	7.51	–	–	–	–	7.10	2.06	1.96	–	9.04	4.48	Ma et. al. (2016)
ZSM-5	94.01	0.55	0.16	0.23	–	0.28	–	–	1.48	–	–	–	–	3.57	Jiang et. al. (2021)
Black rice husk	93.70	0.40	0.92	–	–	–	–	–	–	0.03	2.55	–	–	4.40	Kunchariyakun et. al. (2018)
Bagasse ash	68.60	3.97	7.85	–	–	3.16	1.71	–	1.69	1.07	3.92	–	–	5.22	
Carbide slag	2.57	1.88	65.03	0.09	–	–	–	–	0.17	0.09	–	–	–	28.31	
Quartz tailing	93.23	1.68	0.33	0.56	–	–	–	–	0.14	–	0.64	–	–	0.78	Jin et. al. (2016)
Phospho-gypsum	10.64	1.22	25.39	0.54	–	–	–	–	0.19	0.23	0.50	–	–	22.91	
Quartzite	97.58	0.31	0.14	1.20	–	–	–	–	0.10	0.10	0.03	–	–	0.03	Albayrak et. al. (2007)
Glass cullet	67.1	0.90	7.4	0.20	–	–	–	–	4.2	19.4	–	–	–	–	Walczak et. al. (2015a)
Hematite tailing	24.4	10.95	6.2	44.52	–	–	2.78	–	0.99	0.28	–	–	0.24	6.95	Zhao et. al. (2012)
Copper tailing	44.52	5.36	13.56	1.94	–	–	–	–	19.92	1.00	1.20	–	–	9.26	Huang et. al. (2012)
Blast furnace slag	32.7	15.4	38.79	0.4	–	–	–	–	8.97	0.23	0.36	–	–	0.76	

Abhilasha *et al. Int J Concr Struct Mater*   (2023) 17:6

Page 8 of 22

been used to enhance the properties of AAC (Pehlivanlı et al., 2015, 2016).

Result shows that both type of fiber additives, i.e., hydrophilic, and non-hydrophilic enhanced the flexural and compressive strengths of AAC. Hydrophilic additives are more effective than their respective non-hydrophilic fibers. Compressive and flexural strengths are increased more in this case; whereas, all other fiber substitution enhanced the modulus of rupture of concrete more than the compressive strength, the order of which was as follows: kaolin fiber < basalt fiber < polypropylene fiber < carbon fiber (Laukaitis et al., 2009).

The results of microstructural analysis of FRACs using scanning electron microscope (SEM) showed that the carbon and polypropylene fibers are chemically inert with the hardened concrete matrix. Therefore, FRAC using these fibers can resist the erosion of alkaline mortar media. So it will not be chemically damaged, will not lose its flexibility, and when destructive force is applied to the concrete, they will slide in the matrix of the hardened binder**.** Hence, flexural and compression strength of concretes generally increases in these cases (Laukaitis et al., 2009; Pehlivanlı et al., 2015); whereas, the filaments of fibers like basalt and kaolin fibers chemically react with the binder of concrete. Consequently, they will not slide in the mixture when the concrete is destroyed or when the destructive forces are applied. Due to the chemical reactions, only little increment in the compressive and bending strength of the concrete is observed (Laukaitis et al., 2009).

Experimental examination of fiber reinforcement concluded that the thermal behavior of fiber incorporated AAC linearly varies with thermal properties of the added fibers (Tanyildizi, 2008). AAC reinforced with basalt fiber gives the lowest thermal resistivity. But AAC reinforced with carbon fiber shows higher modulus of rupture and compressive strength. SEM analyses of polypropylene, glass, basalt, fiber undoped AAC and AAC reinforced with carbon fiber are shown in Fig. 4 (Pehlivanlı et al., 2016). Microstructural analysis was obtained using fiber undoped AAC as reference. Fig. 4a shows the C-S-H (tobermorite) crystals of the control sample at (5000×) magnification along with reference sample at (35×) magnification. It was observed that the sizes of pores were varying from 1 and 1.5 mm. In SEM image of basalt FRAC (Fig. 4b), between AAC and basalt fiber (bond produced by the fiber and AAC) adherence compliance was developed. Small quantity of tobermorite gels also visible in the image. In polypropylene FRAC image (Fig. 4c), between AAC and polypropylene fiber adherence compliance was ensured. In cropped carbon FRAC image (Fig. 4d), between AAC and cropped carbon fiber adherence compliance was ensured (Pehlivanlı et al., 2016).

Fig. 4e shows the reinforcement by glass fiber. Also, on the left side, tobermorite (C-S-H) was observed. Reinforcing of AAC with fiber microstructure analysis seems to be strengthen the adherence.

Graphical representation of few desirable properties is shown in Fig. 5. From the graph, it can be easily concluded that the thermal behavior of with fiber AAC (WF) linearly varies with thermal properties of the added fibers unlike non-fiber AAC (NF). It can also be concluded that flexural strength as well as compressive strength also increased in WF when compared to NF. The bulk density was increased in the AAC mix with/without fiber addition.
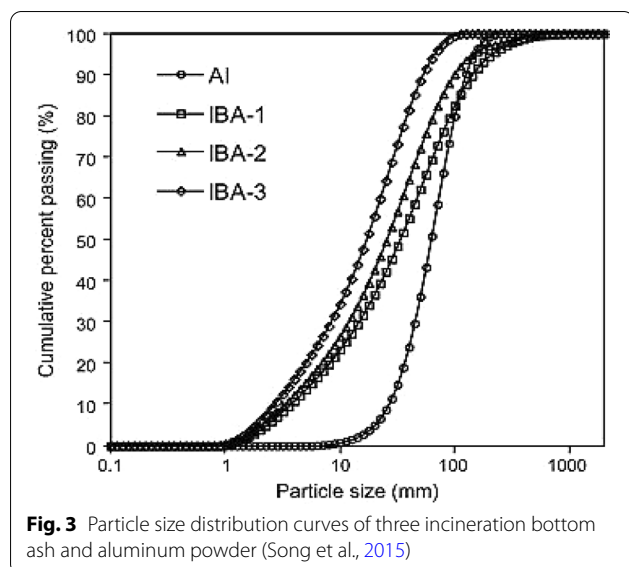
2.5 Hydrophobic Agents

Addition of suitable hydrophobic agents enhanced the strength characteristics of the AAC. This leads to enable its suitability in various field of civil engineering, such as bridge, hydraulic structures, etc. The effect of inclusion of hydrophobic products in preparation of AAC is discussed in this investigation. It has been found that various material properties significantly change at the same time, such as compressive and bending strengths. Also, important effect takes place on reducing water absorption capacity, which play important role in building construction and subsequently enhanced freeze–thaw resistance, carbonation resistance, and chloride ion penetration (Beben and "Zee" Manko, 2011).

2.6 Superplasticizer

By chemical nature, superplasticizers are water-soluble polymers (Dziekan et al., 2011). They contain sulfonated and carboxylated macromolecules and referred as high-range water reducers in concrete. Reduction of the amount of water in the mix is crucial for decreasing the capillary porosity of the hardened cementitious materials. The second important function of a superplasticizer is to retain the specified consistency of concrete at fresh state for a given course of time, even at feasible water/binder ratio (Dziekan et al., 2011). Superplasticizers based on polycarboxylates are useful to influence the properties of AAC. Poly-carboxy, carboxylic groups and polyether contains plasticizers having more solubility in the water.

Solutions of water in which 30% (by wt.) plasticizer are added as an admixture, were applied to concrete (Zeminian et al., 2018). Samples concrete are based on calcium oxide, gypsum and, fly ash as binders and an aggregate. Foam–gas–silicate (FGS) technique was used to form concrete in this study. Mixtures containing superplasticizers as well as mixtures without containing superplasticizers were autoclaved, and then characterized. The

Abhilasha *et al. Int J Concr Struct Mater* (2023) 17:6

Page 9 of 22

Fig. 3 Particle size distribution curves of three incineration bottom ash and aluminum powder (Song et al., 2015)

samples with superplasticizers were enabled to decrease water requirement by 20% and showed 10% higher density, and about 20% higher compressive strength compared to the samples without plasticizers (Zeminian et al., 2018). Phase analysis did not show any differences between these two concrete samples. All samples contained tobermorite phase, and the C-S-H phase. It is important to note that there is not any significant effect on chemical and mineralogical composition of AAC on addition of superplasticizer (Kerienė et al., 2013).

3 Preparation Method of AAC
In the physical stage of mix proportions of AAC, calcareous materials and siliceous materials, the dosage of air-entraining agent (Al powder), initial water temperature, and water solids ratios (W/S) are the major parameters that should be predetermined. The range of bulk (Ca/Al+Si) ratio opted by many researches are varying from 0.48 to 0.83 (Bonakdar et al., 2013; Laukaitis et al., 2009; Pehlivanlı et al., 2016; Qu & Zhao, 2017; Walczak et al., 2015a), whereas binder (cement and lime)/fine aggregate ratio lies as 1:1–1:2 (Qu & Zhao, 2017). The water solids ratios are the ratio of the weight of water, required for mix formation to the weight of solid, required for the formation of mixture. W/S ratio can change depending on the fluidity of the slurry, and hence varies with constituents and mix proportion. At lower W/S ratio, higher viscosity with rapid hardening will slow down its smooth swelling because of increased cohesive forces (Laukaitis et al., 2009).

Pore structure, such as distribution and pore size relates the variation in the volume of AAC slurry which is essentially control by W/S ratio (Laukaitis et al., 2009).

At a very higher W/S ratio, the segregation in the slurry occurs at different location and the hardening rate becomes slow. Hence, gas is not entrapped properly and tends to move upward which consequently generates interconnected pores. This distribution of uneven pores in the direction of expansion is known as anisotropy (Qu & Zhao, 2017). The setting rate of slurry and gas-formation rate is influenced by the initial water temperature which is responsible for the balance between these two. Reasonable water temperature increases the temperature of slurry about 70–80 °C at room temperature which consequently provides satisfactory pore size (Ma et al., 2016; Qu & Zhao, 2017). The density of AAC can be adjusted by the dosage of aluminum powder and the range of aluminum powder lies between 0.1 and 0.25% of the weight of binder (Bonakdar et al., 2013; Hussin et al., 2010; Kunchariyakun et al., 2015; Rahman et al., 2021; Wang et al., 2016; Zafar et al., 2020). With steam curing in autoclave treatment, the transformation of an originally formed C-S-H phase takes place into tobermorite ($5CaO·6SiO_2·5H_2O$) by reacting with dissolved silica. This hydrated product provides smaller shrinkage and higher compressive strength at a lower density. Gyrolite ($Ca_4(Si_6O_{15})·(OH)_2·3H_2O$) was formed when finer quartz is utilized for preparation of AAC at higher autoclaving time (Albayrak et al., 2007). On increasing the autoclaving pressure (i.e., > 0.8 MPa) tobermorite developed well, whereas when the autoclaving pressure was more than 1.2 MPa other hydrothermal products were also formed which had lower strength (Serhat Baspinar et al., 2013; Cong et al., 2016; Zhao et al., 2012). Tobermorite appears at nearly 2 h of autoclaving and profound up to 6–8 h and further, no formation takes place on increasing time (Narayanan & Ramamurthy, 2000; Wang et al., 2016). The process of AAC preparation is described in Fig. 6 (Hamad, 2014).

4 Physio-mechanical Properties
4.1 Density
Bulk density affects numerous behaviors of AAC, such as dry shrinkage, compressive strength, and thermal conductivity (Tada, 1986). The specific gravity of constituent materials and quantity of air-entraining agent are the factors that closely controlled the bulk density (Karakurt et al., 2010; Kunchariyakun et al., 2015; Song et al., 2015). As the density control the various physical properties of AAC, it is essential to specify the density with respect to the moisture condition, i.e., at equilibrium with the atmosphere or oven-dry condition. AAC produced from autoclaving may be 15 to 25% more heavier than oven treated AAC (Narayanan & Ramamurthy, 2000). On increasing the duration of autoclave (i.e., > 8 h), bulk density slightly increases because more hydration products
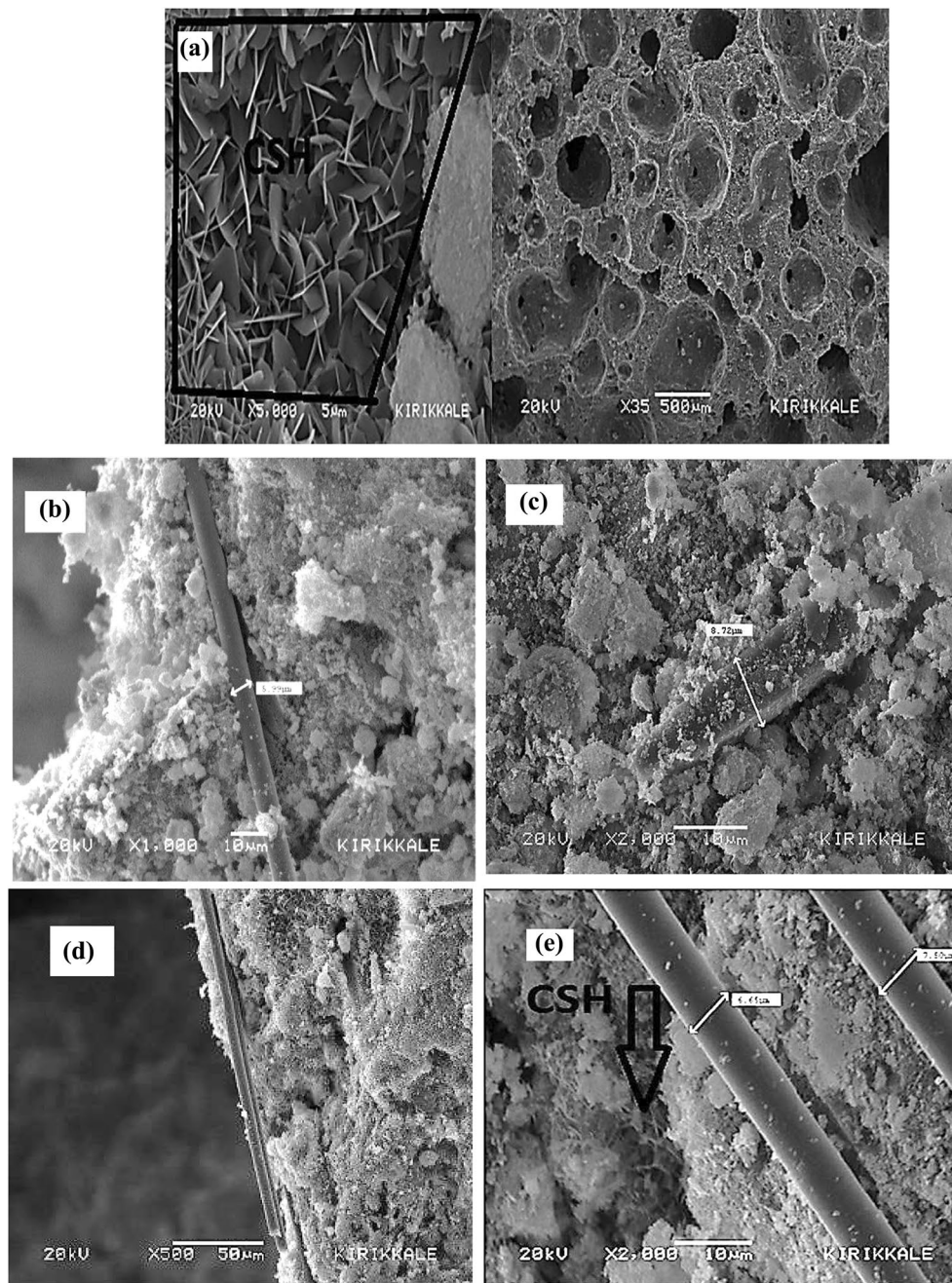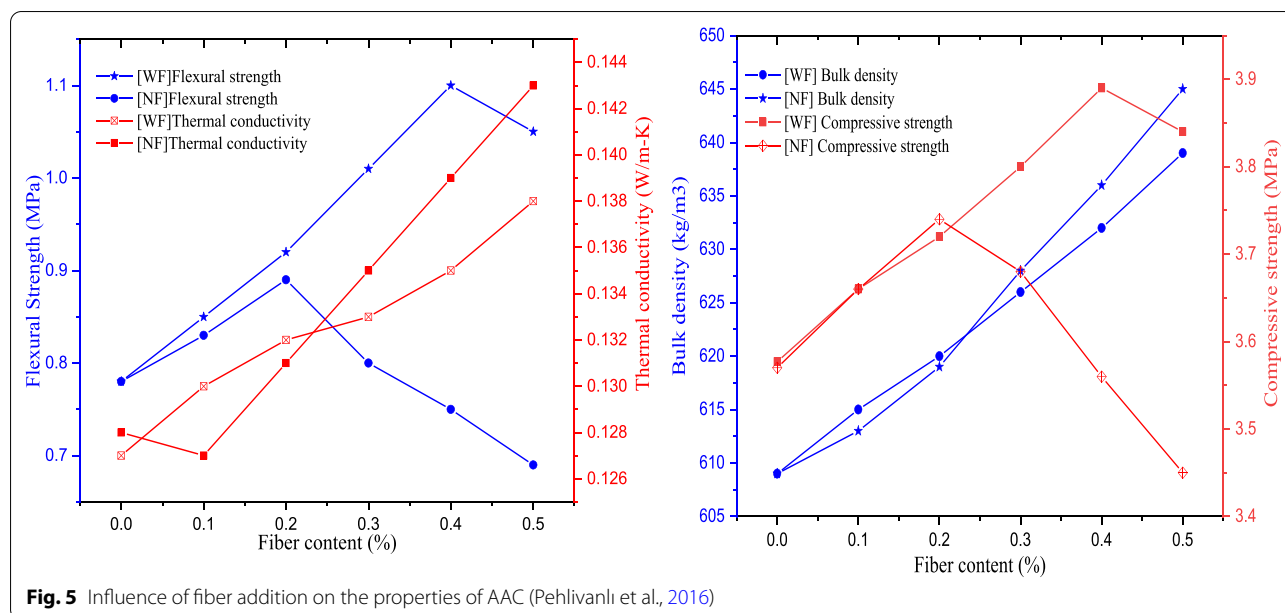
Abhilasha *et al. Int J Concr Struct Mater*   (2023) 17:6

Page 10 of 22

Fig. 4 SEM image analysis of **a** reference AAC; **b** basalt FRAC (×1000); **c** polypropylene FRAC (×2000); **d** cropped carbon FRAC (×2000) and **e** glass fiber FRAC (×500) (Pehlivanlı et al., 2016)

were formed (Narayanan & Ramamurthy, 2000; Karakurt et al., 2010).

AP reacting with lime results in a decrement in density, consequently reducing the strength of AAC. To compensate this decrement in strength, marble waste used as substituents of cement which fill the micro-pores created during aeration reaction hence enhanced the strength of AAC. Hence reutilization of industrial waste helps to the development of energy-efficient concrete (Perumalsamy et al., 2018). Fig. 7 shows graphical representation of bulk density. AAC samples with RHA showed gradual decrement in the density (Kunchariyakun et al., 2015). Responsible cause for this decrement was the lower specific gravity of RHA (Kunchariyakun et al., 2015); whereas, the

Abhilasha *et al. Int J Concr Struct Mater*   (2023) 17:6

Page 11 of 22

Fig. 5 Influence of fiber addition on the properties of AAC (Pehlivanlı et al., 2016)

sudden decrease was observed in the density of BA substituted AAC samples (Kunchariyakun et al., 2018). This was due to the nonpolar surface and retardation effect of presented unburned carbon in BA. At 20% of optimum replacement of sand by granite dust, density of AAC was increased by 13.45% (Zafar et al., 2020). Responsible cause for this increment was the formation of higher density tobermorite crystals, instead of hexagonal Portlandite crystals (Zafar et al., 2020). The bulk density was decreased by 12% when quartz sand replaced with 5% perlite waste; whereas, density was decreased by 45% quartz sand replaced by 40% perlite waste (Różycka & Pichór, 2016).

4.2 Compressive Strength

The measurement of resistance which is offered by walls of pores to stress is known as compressive strength. Many factors can affect the compressive strength, such as pore size distribution with the number of pores and the hydrothermal products (such as C-S-H) formed by the binder (Tada, 1986). However, the porosity has imposed more effect on this mechanical property. Porosity also affects density, as increase in the porosity, density reduces. However, compressive strength is not solely dependent on porosity, but pore size can also influence it. Smaller pores lead to higher compressive strength in comparison to larger pores (Hoff, 1972; Tada, 1986); whereas reduction in density leads to the decrement in compressive strength (Albayrak et al., 2007; Alexanderson, 1979; Bonakdar et al., 2013; Holt & Raivio, 2005; Hu et al., 1997; Kunchariyakun et al., 2018; Narayanan & Ramamurthy, 2000;

Petrov & Schlegel, 1994; Song et al., 2015; Wongkeo & Chaipanich, 2010; Wongkeo et al., 2012).

Microstructure and ingredients also influence the compressive strength. W/S ratio predicts the amount of water which is very important to maintain the density as well as compressive strength. Higher compressive strength is the result of smaller microscopic pores which can be derived from smaller values of the W/S ratio (Kunchariyakun et al., 2015; Song et al., 2015). Tobermorite crystals are majorly responsible for the compressive strength of AAC. Higher compressive strength and more crystalline phases are correlated to each other hence basic proportioning should be optimal for larger tobermorite crystals (Thongtha et al., 2014). Low values of the C/S ratio result in the creation of very poor-quality crystalline phase as well as not facilitates the formation of Tobermorite crystals. Hence, to prevent these outcomes the range of the C/S ratio should lie at 0.8–1.0 (Mostafa, 2005). Quartz sand is higher in the percentages of silica in comparison to river sand thus the estimated addition of sand is bound to 20% only, whereas an increment in compressive strength has been observed from 2.2 to 3.74 MPa on increasing the quantity of quartz sand (Cicek & Tanrıverdi, 2007).

From Fig. 8, it can be concluded that addition of waste can enhance the strength of AAC. Optimal range for the addition of various wastes to improve the compressive strength of AAC is 30–40%, as shown in the graph. At 30% of optimal replacement by different wastes, such as black rice husk ash (Kunchariyakun et al., 2018), bottom ash (Kunchariyakun et al., 2018), and sugar sediment (Thongtha et al., 2014), compressive strength increases by 46%, 26% and 18%, respectively. Beyond 40% addition
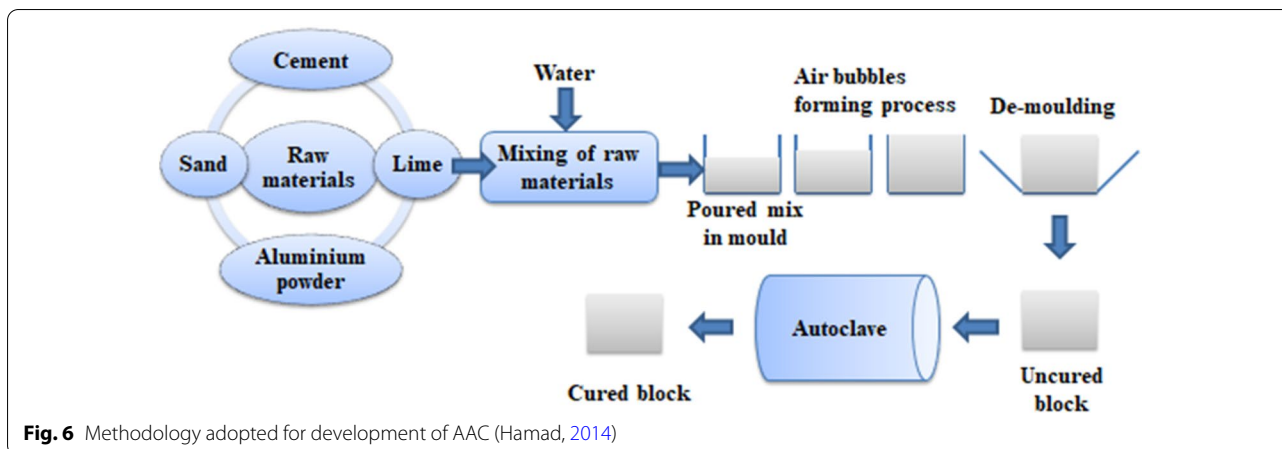
Abhilasha *et al. Int J Concr Struct Mater*   (2023) 17:6

Page 12 of 22

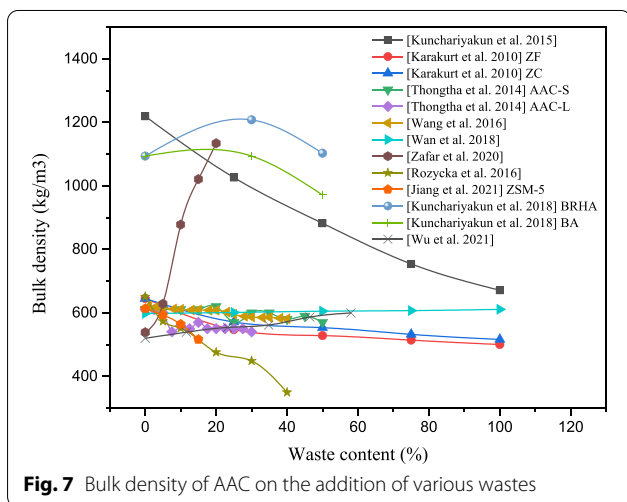**Fig. 6** Methodology adopted for development of AAC (Hamad, 2014)

Fig. 7 Bulk density of AAC on the addition of various wastes

of waste shows no improvement on the compressive strength and it decreases gradually. As specific strength is defined as strength per unit density, compressive strength increases with increase in density and vice-versa. From Fig. 8b, it can be observed that optimal addition of various kinds of wastes (by 20–40%), such as black rice husk ash (Kunchariyakun et al., 2018), bottom ash (Kunchariyakun et al., 2018) can improve the specific strength of AAC.

4.3 Flexural Strength

Flexural strength is the measurement of bending strength of beams or slabs of AAC when exposed to a transverse load at the mid-span of the beam and its value is about 17–34% of their compressive strength (Hu et al., 1997). Comparison between the properties of AAC and FRAC was studied. It was concluded that AAC has slightly higher maximum flexural stress than FRAC (Dey et al., 2014); whereas deflection and toughness capacity are

reported higher in FRAC than AAC due to the presence of polypropene fiber (0.5% by weight) which provides bridging to cracks (Song et al., 2015). Fig. 9 shows that at 50% replacement of ZC (coarse zeolite 0.5–1 mm) in the formation of AAC provides max strength. On the other hand, ZF (fine zeolite 100 μm) decreased the strength due to lower particle size and retardation effect of pozzolonic materials (Karakurt et al., 2010). At 20% optimal replacement of sand by waste granite dust, flexural strength was increased by 50% (Zafar et al., 2020).

4.4 Drying Shrinkage

The process of drying leads to dimensional changes responsible for inducing cracks in the structure. AAC shows high drying shrinkage which is the result of the specific surface of pores, high porosity, and absence of aggregates. Drying shrinkage of porous building material is explained by capillary tension theory which stated that water experiences stress in the micro-pores which creates attraction between the walls of the pore (Nielsen,1983; Ramamurthy & Narayanan, 2000). AAC has less drying shrinkage when compared to NAAC due to the conversion of set cement gel into microcrystalline form after autoclaving (Alexanderson, 1979; ACI 516, 1965).

As cement is fine, it therefore provides a large surface area to evaporate adsorbed water and hence higher drying shrinkage can be observed. The increment in lime/cement ratio increased the quantity of fines in the mixture which consequently increases the drying shrinkage. So limiting the incorporation of lime in the mix prevents the increment in drying shrinkage. Fly ash also increases the drying shrinkage due to the presence of a higher surface area (Lam et al., 2018). The quantity of air-entraining agent, superplasticizers, and silica fumes has no influence on drying shrinkage (Ramamurthy & Narayanan, 2000);

whereas the incorporation of alumina-rich substances, such as bauxite, alumina-rich cement and blast furnace slag can decrease the percentage of drying shrinkage by 30–100% because of the development of a greater number of tobermorite (Alexanderson, 1979).

The shrinkage mechanism of AAC is still unclear. It has not been thoroughly explored for the wide range of saturation conditions to dry conditions at various range of relative humidity (RH) (Lam et al., 2018). Drying shrinkage of AAC has been studied at lower and higher value of RH. Result shows that at higher RH (>65%), capillary tension theory plays important role for the drying shrinkage mechanism; whereas at lower RH (<65%) the shrinkage of AAC has a linear connection with the surface energy change. It has been determined that the primary factor for AAC to shrink under low RH circumstances (RH 65%) is a shift in the surface free energy (Lam et al., 2018).

4.5 Water Absorption

High porosity is the main characteristic of AAC which is mainly responsible for high moisture absorption of AAC (Jerman et al., 2013). Water absorption is basically worked from two channels, i.e., capillary pores and artificial air pores. The volume of capillary pores does not vary so much but as the volume of artificial air pores increases, average length for water migration also increases in the material. Moisture absorption in air pores is resulting from the capillary rise which can be observed when any porous material comes into the contact of water and can be explained by the following relationship:

$$\Delta M = CF\sqrt{t},$$

where 'F' is absorbed water per surface area with time (t); 'C' is the capillary coefficient and depends on number of participated pores during the suction process. Moisture condition plays a decisive role in water absorption (Lam et al., 2018). Water vapor diffusion increases in the dry state because all pores are vacant in the dry state; whereas, in the regions where humidity is high, the capillary condensed water can fill some pores due to which these pores will not contribute to water vapor diffusion, and consequently water moves in it through the capillary forces only (Prim & Wittmann, 1983). Fig. 10 shows
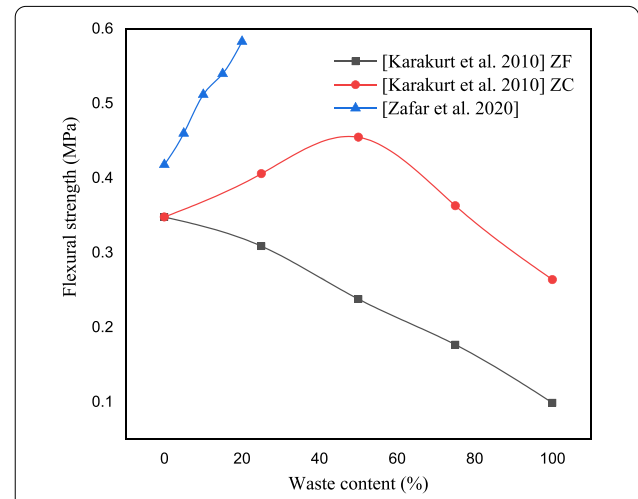
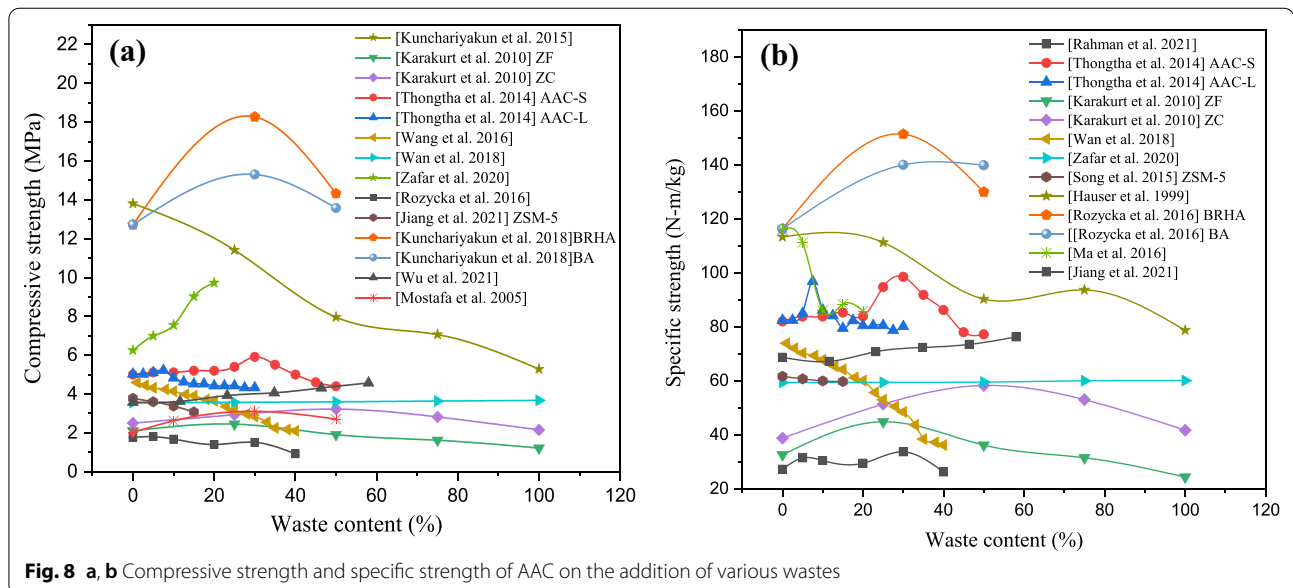**Fig. 9** Flexural strength of AAC on the addition of various wastes

Fig. 8 a, b Compressive strength and specific strength of AAC on the addition of various wastes

graphical representation of water absorption using different wastes, such as sugar sediments (Thongtha et al., 2014), waste granite dust (Zafar et al., 2020) and, stone sawing mud (Wan et al., 2018). On increasing the percentage of various wastes, water absorption was constant. However, decrement in the water absorption is the result of lesser porosity. Water absorption gradually decreased up to 8% when sand is replaced by SSM from 10 to 100% (Wan et al., 2018).

5 Microstructural Analysis

5.1 Mineralogy

Alite and belite are the major C-S-H phases of Portland cement. The reaction of alite with water is relatively faster than belite leads to development of early strength in concrete. Belite reacts slowly in initial stages, but in later ages it can significantly impart strength in concrete (Karakurt et al., 2010). Autoclaving process limits the formation of Portlandite as a result of development of stable C-S-H, which have similar properties alike tobermorite natural mineral (characterized by a 11.3 Å basal reflection and discovered in 1880 by Heddle). As the autoclaving time increases, initial crystalline phases produced by various components (Isu et al., 1995; Karakurt et al., 2010; Kikuma et al., 2011; Klimesch et al., 1996). The literature study on XRD has confirmed that C-S-H, tobermorite, and other crystalline systems are the main mineralogical constituent of AAC (Albayrak et al., 2007; Hauser et al., 1999; Huang et al., 2012; Karakurt et al., 2010; Kunchariyakun et al., 2015; Mostafa, 2005; Yang et al., 2013). Earlier studies showed that the C/S ratio determines the texture and micro-morphology of crystalline phases like tobermorite crystals (Hong & Glasser, 2004; Mostafa, 1995; Mostafa et al., 2001; Pellenq et al., 2009; Sato & Grutzeck, 1991; Taylor, 1997).

The optimal C/S range for the formation of tobermorite has been reported by previous works, which shows that the range lies between 0.8 and 1.0 (Kunchariyakun et al., 2015; Mostafa, 2005). At a higher C/S value (> 1), tobermorite crystals of needle-shaped were formed; whereas at lower C/S value (< 1), crumbled foil-like and plate-like tobermorite crystals were formed but at very less C/S value (< 0.8), grass-like C-S-H was observed which can be easily convert in tobermorite crystals due to having short silica chains. (Kunchariyakun et al., 2015, 2018; Papatzani et al., 2015; Sato & Grutzeck, 1991).

The effect of waste granite dust (WGD) inclusion in AAC has also been studied (Zafar et al., 2020). High-quartz sand is partially replaced by WGD in various percentage of replacement, such as 5, 10, 15, and 20%. In this research, the energy dispersive X-ray (EDX) test on AAC result showed that the C/S ratios of the crystalline phases comes out to be 0.99, 0.94, and 1.40 for WGD10

mix, WGD20 mix, and CM, respectively (Zafar et al., 2020). For WGD10 mix, foiled tobermorite (plate-like/crumble) (Fig. 11c), and for WGD20, C-S-H gel (Fig. 11b) was observed; whereas microstructure of CM mixes the calcium hydroxide hexagonal plate-like morphology was observed (Fig. 11a). All crystals are shown in Fig. 11 (Zafar et al., 2020).

5.2 X-ray Diffraction Analysis

Solid crystalline phases of specimens formed by using wastes were analyzed by XRD. Fig. 12 represents the diffraction patterns of AAC after 8 h and 18 h of autoclaving time with and without waste (Kunchariyakun et al., 2015). Fig. 12a shows the peak of quartz, $Ca(OH)_2$ and tobermorite crystals with high intensity. As RHA introduced in control mix, peak intensity of quartz and $Ca(OH)_2$ was decreased. As the substitution of RHA reached up to 100%, peak of quartz has disappeared; whereas, the peak intensity of tobermorite was increased on RHA substitution. Decrement in the peak of $Ca(OH)_2$ concluded that silica which present in RHA is highly reactive and readily consumed $Ca(OH)_2$ to produce C-S-H. However, there is no effect on tobermorite formation when temperature was increased from 8 to 18 h (Fig. 12b) (Kunchariyakun et al., 2015). XRD of AAC (Fig. 12d) with stone sawing mud concludes that tobermorite is main constituent (Wan et al., 2018) and its peak intensity was increased as compared to normal AAC samples (Fig. 12c). XRD graphs of AAC with ZSM-5 waste are shown in Fig. 12e, f. It shows that sample produced with 15% ZSM-5 (or ZN15) has the highest crystallinity peak, as shown in Fig. 12e. As the time of autoclaving increased, peak of CH, mullite was
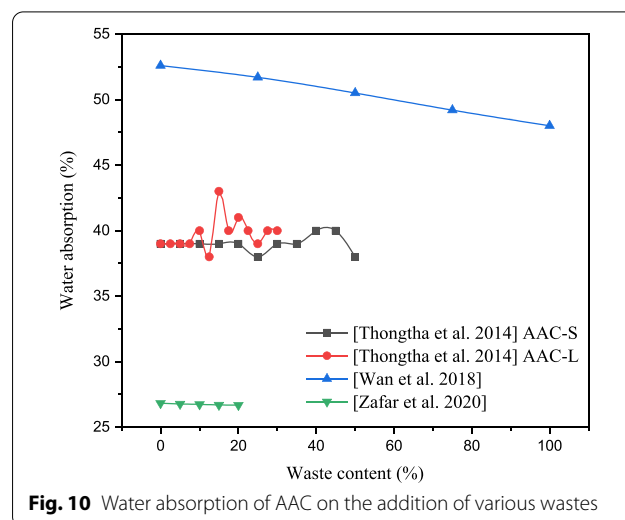

Fig. 10 Water absorption of AAC on the addition of various wastes

decreased in Fig. 12f (Jiang et al., 2021). Tobermorite was formed predominantly after 2 to 8 h.

5.3 Pore Structure

High porosity (which covers the range from 65 to 90%) is the main characteristic of AAC. Due to this property, density and compressive strength of AAC is comparatively low with respect to normal-weight concrete (Bonakdar et al., 2013; Thongtha et al., 2014). There are at least two types of pores in AAC, which are called "macro-pores" and "micro-pores". Macro-pores are pores with diameters more than 50 nm and micro-pores have pore sizes lower than 2 nm (Lam et al., 2018). The other one is called "meso-pores" and they exist between the gaps of these two ranges. The pore distances of air pores in AAC may range from one millimeter down to zero which means the pores touch each other or are even interconnected. The pore size in AAC is always in the millimeter range, mostly having diameters in the range between 0.5 and 3.0 mm as shown in Fig. 13a (Schober, 2011).

The pore size distribution is commonly a mono modal and narrow one and it is primarily a matter of air-entraining agent or method by which medium size of air pores will be generated in AAC. The air pores contribute between 25 and 70% to the total volume of pores introduced in AAC during the manufacturing process (Schober, 2011). The expanding crack structure is a significant pore structure element in AAC material made with aluminum as shown in Fig. 13b. The cracks own a preferred orientation that they lie horizontal when the rising direction is upward and mostly are interconnecting the air pores (Petrov & Schlegel, 1994; Schober, 2005, 2011).

6 Functional Property: Thermal Conductivity

AAC has very low thermal conductivity due to its cellular structure and it ranges from 0.1 to 0.7 W/mK in the density range of 400–1700 kg/m^3; whereas for normal-weight concrete value of thermal conductivity lies between 1.6 and 2.0 W/mK (Dey et al., 2014; Thongtha et al., 2014). Many factors can influence the thermal conductivity, such as pore structure, density, etc. However, thermal conductivity has largely been influenced by density. On the decrement of density, thermal conductivity also decreases. On the other hand, density and porosity both are inversely proportional to each other. More porosity % results in more entrapped air in the pores and hence less density and more thermal insulation have been observed. On increasing porosity from 50 to 70%, decrement of thermal conductivity as 0.22–0.08 W/mK, was observed (Albayrak et al., 2007; Dey et al., 2014; Hu et al., 1997; Jerman et al., 2013; Kreft et al., 2011; Kunchariyakun et al., 2015; Schober, 2005; Topçu & Uygunoğlu, 2007).

Depending on the phase structure, thermal conductivity also varies. AAC with fly ash has a lower value of thermal conductivity than AAC with Quartz sand because they both have different hydrated phases, and also fly ash particles have microporous structures as compared to Quartz sand (Choo et al., 2021). Fly ash has glass phases whereas quartz sand has crystalline phases. Since, fly ash has a high glass concentration. Therefore, it is possible to see distinct phase compositions, such as tobermorite-like fiber, gel C-S-H, or hydrogarnets, due to high Al_2O_3 content within fly ash incorporated AAC. While, only a tobermorite-like plates can be seen in the sand incorporated AAC (Walczak et al., 2015b). Also, apart from the above, as fly ash comprises 60–85% glass, 10–30% crystalline compound and around 5% unburned carbon. Particles of carbon are generally cellular (>45 μm). Studies
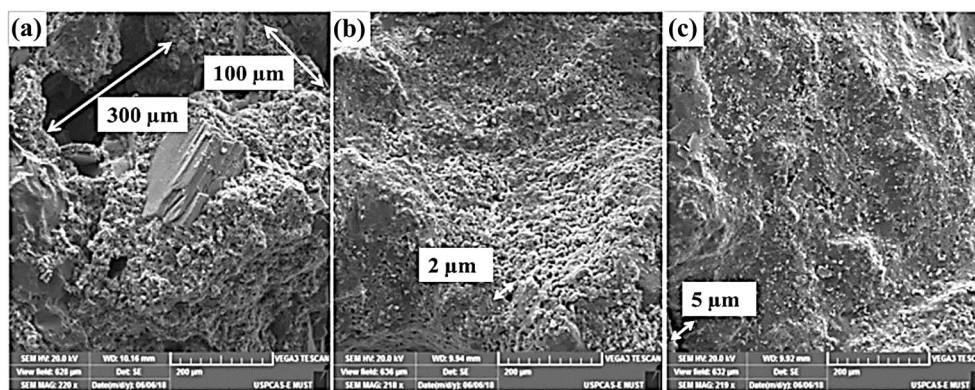

Fig. 11 Surface texture of granite dust incorporating AAC. **a** Control mix; **b** WGD20 and **c** WGD10 (Zafar et al., 2020)
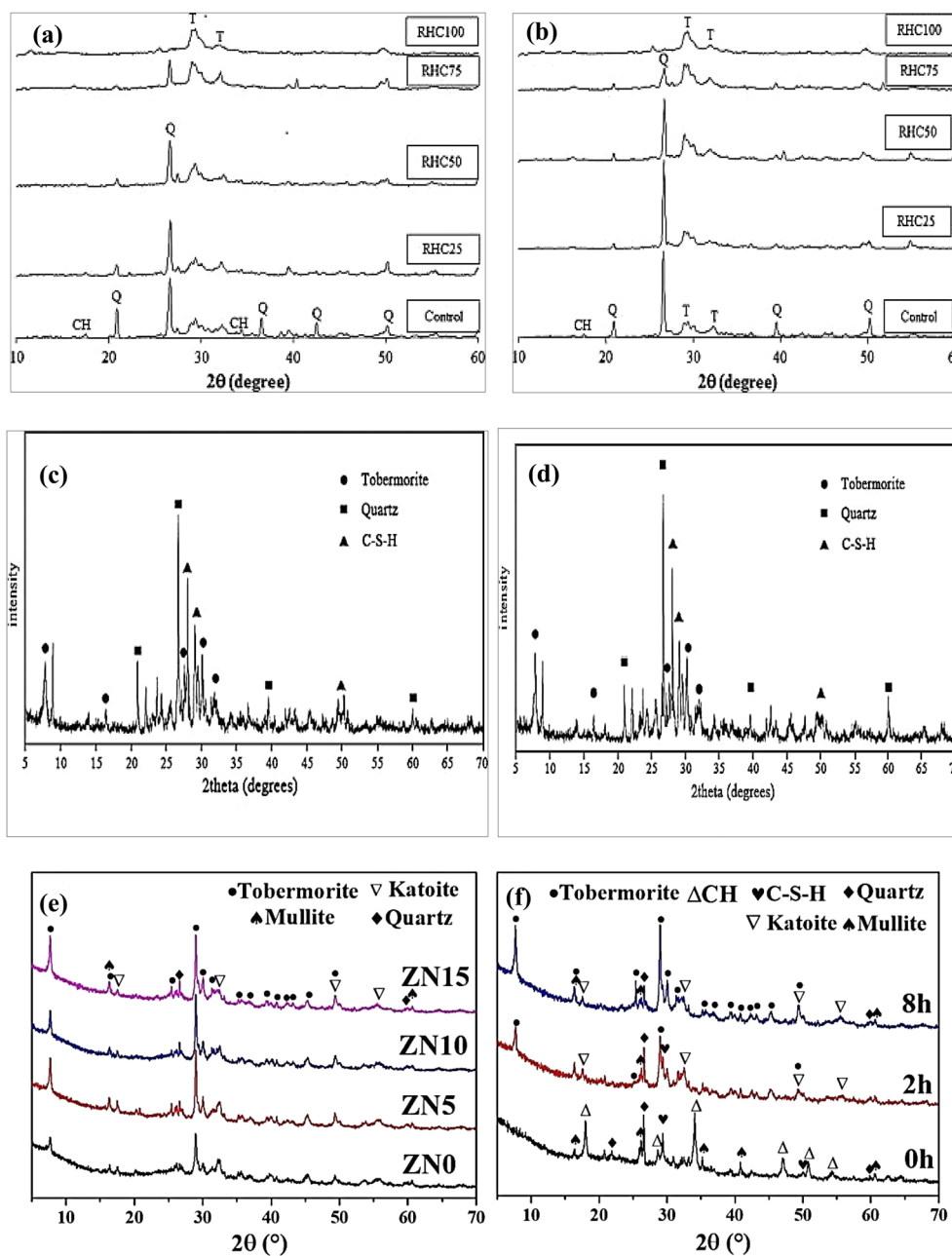
Fig. 12 XRD patterns of rice husk ash AAC samples: **a** at 8 h of autoclaving time and **b** 18 h of autoclaving time (Kunchariyakun et al., 2015). XRD curves of **c** normal AAC sample and **d** stone sawing mud AAC sample (Wan et al., 2018). XRD patterns of AAC **e** at different percentage of ZSM-5 waste and **f** 15% ZSM-5 AAC sample at different autoclaving time (Jiang et al., 2021)

on particle size distribution reveal that fly ash contains particles ranging from nearly 1 μm to 100 μm (Mehta & Monteiro, 2013). Most of the particles in fly ash occur as solid spheres of glass. Sometimes a small number of hollow spheres, called cenospheres (completely empty) and plerospheres (packed with numerous small spheres), may also be present. Presence of these hollow spheres in

fly ash increases the porosity in the fly ash incorporated AAC. As the thermal performance of AAC is directly related to the porosity, the larger the porosity, the lower the thermal conductivity (Chen et al., 2021; Kumar, 2021). Thus, due to the above reasons, fly ash induced AAC has lower thermal conductivity as compared to AAC with quartz sand.

Low specific gravity substances reduce thermal conductivity, e.g., coal bottom ash (39% reduction), rice husk ash (29% reduction), perlite waste (41% reduction), and natural zeolite (47% reduction) (Karakurt et al., 2010; Kunchariyakun et al., 2015; Kurama et al., 2009). Thermal conductivity depends on the water content, i.e., by increasing the water content by 10%, thermal conductivity can increase about 0.04–0.05 W/mK (Campanale & Moro, 2016; Campanale et al., 2013; Collet & Pretot, 2014; Jerman et al., 2013; Jin et al., 2016). Autoclaving has no effect on thermal conductivity (Narayanan & Ramamurthy, 2000; Karakurt et al., 2010). Fig. 14 shows the graphical representation of thermal conductivity, waste content and bulk density. It shows that on increasing the different waste content thermal conductivity of AAC decreased. So, AAC can be used for thermal insulation in construction.

7 R&D at CSIR-CBRI

Earlier, R&D work has been done on Lightweight Concrete by CSIR—Central Building Research Institute (CBRI) (Lakhani & Kumar, 2015; Kumar, 2020, 2021; Kumar & Lakhani, 2021; Kumar & Srivastava, 2022; Kumar et al., 2021a, 2021b). Limestone slurry has been used for the development of Cellular Lightweight Concrete (CLC) blocks of density ranging from 650 to 1200 kg/m^3 (Kumar et al., 2018). Generally, cement, fly ash and natural river sand are the basic constituents for the formation of CLC blocks. For the generation of foam, natural protein based foaming agent was used in the ratio of 1:20 (foaming agent and water). Limestone slurry being rich in silica content, was used for the replacement of natural river sand. 50% optimized replacement of natural river sand was done by limestone slurry. Various physico-mechanical properties of the developed CLC blocks were determined. It was found that there was enhancement in compressive strength and performance factor of CLC blocks.

At present, CSIR-CBRI has initiated the work on the development of AAC blocks by using different waste materials like marble slurry, fly ash, industrial wastes, etc. Fig. 15 shows the laboratory preparation of AAC blocks at CSIR-CBRI. Targeted features to be achieved are as per IS 2185 (Part-3), i.e., density and compressive strength should be in range 451 to 1000 kg/m^3 and 2.0 to 7.0 MPa, respectively. Thermal conductivity should lie between 0.21 and 0.42 W/mK.

8 Recommendations

- In order to reduce the carbon emission, replacement of cement by different wastes should be acknowledged in the preparation of AAC.
- Impact of various wastes on the acoustic properties of AAC must be studied.
- Utilization of demolished AAC waste should also need attention in construction.
- As micro- and macro-pores are the main characteristic of AAC, therefore how the utilization of different waste affects the porosity of AAC should be studied.
- Stone wastes contain various other components (except quartz) like potassium and soda feldspar. Their involvement in the hydration process is still not much explored.
- Strength of AAC is related to the moisture content. Detailed study of this parameter will be helpful for further research studies.
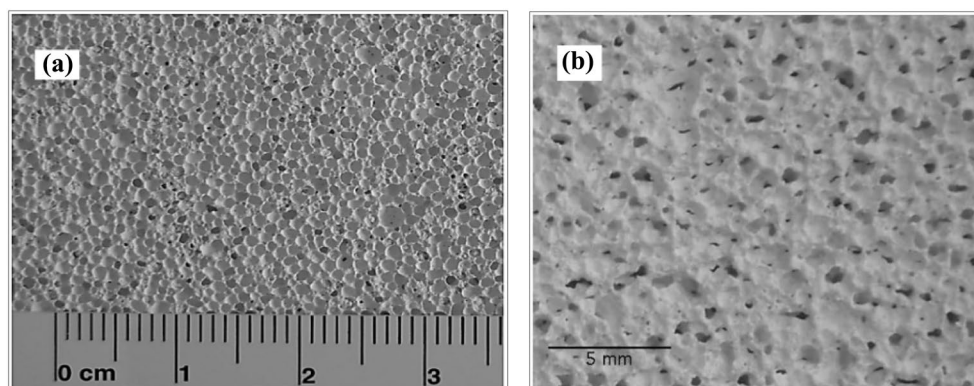

Fig. 13 Pore structure of **a** AAC sample and **b** expanding crack structure of an AAC sample made with aluminum powder as expanding agent (Schober, 2011)

9 Conclusions

The following observations are being provided in light of the many literature studies that were previously mentioned. Autoclaved aerated concrete (AAC) offering a potential solution for dealing with various wastes. While focus on the changes in microstructure and characteristics is important, it is also important to consider the underlying toxicity of waste. Investigations of the microstructure using a scanning electron microscope and an X-ray diffraction study will be useful for determining the pore development and structure of AAC. There is evidence in the literature that properties of AAC can be enhanced by wastes/byproducts according to criteria of affordability and durability. The following findings can be made as a result of the literature review:

- As most of the raw materials of AAC are silicious in nature. It offers wide opportunity for the various silicious waste throughout the world. For e.g., Rice Husk, Natural zeolite and Sugar sediments, etc., highly rich in silica content (>65%) can easily replace natural resources like sand (up to 20–40%).
- As it is light in weight, therefore application becomes very easy. As well as it requires less reinforcement in the foundation work of buildings.
- All the ingredients used in the production of AAC are eco-friendly and utilization of fly ash as one of the constituents is leading it towards greener development.
- The pore size in AAC is always in the millimeter range, mostly having diameters in the range between 0.5 and 3.0 mm.

- Presence of air voids in AAC, provide thermal insulation properties to it. Due to its thermal insulation property, about 50% consumption of building energy reduces. Hence maximize energy efficiency in buildings.
- AAC block generated around 67% less carbon emissions than clay brick.
- AAC can be used in constructions of panel in both load and non-load bearing for walls, roofs, floors, etc.
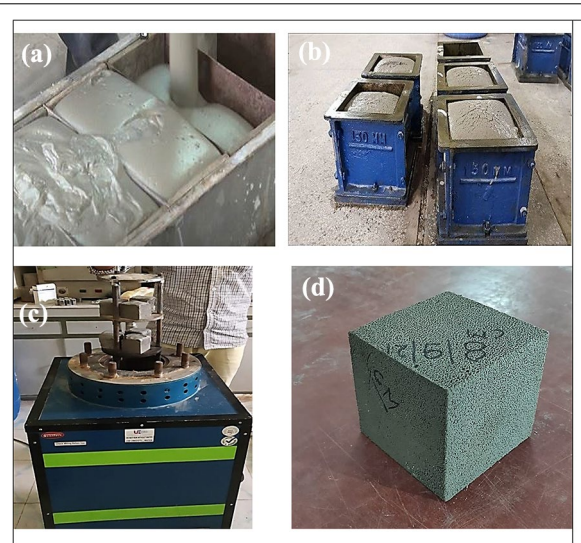- Fiber-reinforced aerated concrete (FRAC) had nearly half compressive strength than that of AAC samples

Fig. 15 Laboratory preparation of light weight concrete. **a** Pouring of mix; **b** expansion of mix; **c** autoclaving of AAC blocks and **d** developed AAC block
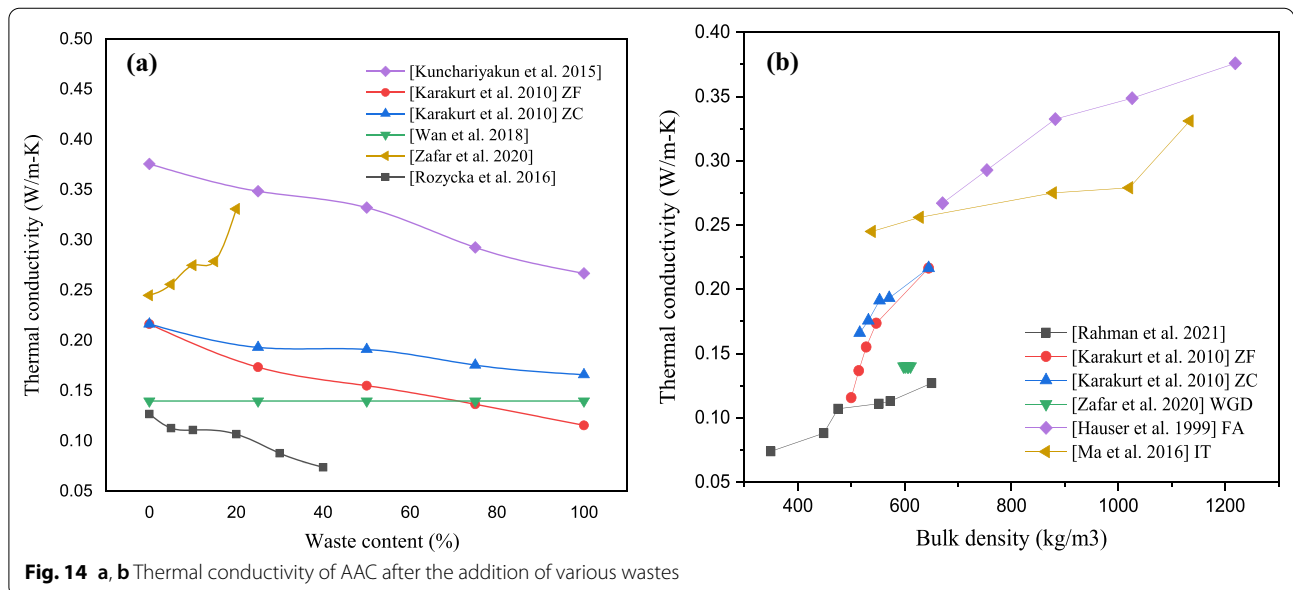

Fig. 14 a, **b** Thermal conductivity of AAC after the addition of various wastes

but flexural strength of FRAC was 100 times greater than that of AAC.

- On increment in the autoclaving pressure (i.e., >0.8 MPa) tobermorite developed well, whereas when the autoclaving pressure was more than 1.2 MPa other hydrothermal products were also formed which have lower strength.
- Tobermorite crystals are majorly responsible for the compressive strength of AAC. Tobermorite appears at nearly 2 h of autoclaving and profound up to 6–8 h and further, no formation takes place on increasing time.
- Preparation of AAC by using different industrial wastes is a great way to cope with the problems which have been generated by the wastes.

Abbreviations
AAC: Autoclave aerated concrete; NAAC: Non-autoclaved aerated concrete; C-S-H: Calcium-silicate-hydrate; RHA: Rice husk ash; IOT: Iron ore tailings; CG: Coal gangue; SSM: Stone sawing mud; OPC: Ordinary Portland cement; SMD: Silica micro-dust; AS: Amorphous silica; CF: Carbon fiber; UIV: Ultrasonic impulse velocity; WGD: Waste granite dust; PPC: Pozzolana Portland cement; AP: Aluminum powder; MSW: Municipal solid waste; IBA: Incineration bottom ash; FRAC: Fiber-reinforced aerated concrete; FGS: Foam gas silicate; BF: Basalt fiber; CM: Control mix; BRHA: Black rice husk ash; BA: Bottom ash.

Acknowledgements
Not applicable.

Author contributions
A: conceptualization/reproducibility of results/experiments, data curation, writing—original draft preparation, writing—review and editing. RK: methodology, validation, formal analysis, Investigation, supervision, formal analysis, writing—review and editing. RL: investigation, supervision, formal analysis. RKM: data curation, methodology, validation, writing—original draft preparation. SK: writing—review and editing. All authors have agreed to the published version of the manuscript. All authors read and approved the final manuscript.

Authors' information
Abhilasha: First Author, Ph.D. Research Scholar, AcSIR-Academy of Scientific and Innovative Research, Ghaziabad, Uttar Pradesh, 201 002, India & Project Assistant, Organic Building Materials (OBM) Group, CSIR-Central Building Research Institute, Roorkee, Uttarakhand, 247 667, India.
Rajesh Kumar: Second Author and Corresponding Author, Senior Scientist & Head, Organic Building Materials (OBM) Group, CSIR-Central Building Research Institute, Roorkee, Uttarakhand, 247 667, India.
Rajni Lakhani: Third Author, Ph.D, Chief Scientist, Organic Building Materials (OBM) Group, CSIR-Central Building Research Institute, Roorkee, Uttarakhand, 247 667, India.
Raghav Kumar Mishra: Fourth Author, Project Assistant, Organic Building Materials (OBM) Group, CSIR-Central Building Research Institute, Roorkee, Uttarakhand, 247 667, India.
Shahnavaz Khan: Fifth author, Project Assistant, Organic Building Materials (OBM) Group, CSIR-Central Building Research Institute, Roorkee, Uttarakhand, 247 667, India.

Availability of data and materials
Not applicable.

Declarations

Competing interests
The authors declare that they have no competing interests.

Author details
[1]AcSIR-Academy of Scientific and Innovative Research, Ghaziabad, Uttar Pradesh 201 002, India. [2]Organic Building Materials (OBM) Group, CSIR-Central Building Research Institute, Roorkee, Uttarakhand 247 667, India.

References
Albayrak, M., Yörükoğlu, A., Karahan, S., Atlıhan, S., Yılmaz Aruntaş, H., & Girgin, İ. (2007). Influence of zeolite additive on properties of autoclaved aerated concrete. *Building and Environment, 42*(9), 3161–3165. https://doi.org/10.1016/j.buildenv.2006.08.003

Alexanderson, J. (1979). Relations between structure and mechanical properties of autoclaved aerated concrete. *Cement and Concrete Research, 9*(4), 507–514. https://doi.org/10.1016/0008-8846(79)90049-8

Alyamaç, K. E., & Aydin, A. B. (2015). Concrete properties containing fine aggregate marble powder. *KSCE Journal of Civil Engineering, 19*(7), 2208–2216. https://doi.org/10.1007/s12205-015-0327-y

American Concrete Institute. (1965). High pressure steam curing modern practice, and properties of autoclaved products. *ACI Journal Proceedings.* https://doi.org/10.14359/7728

Beben, D., & "Zee" Manko, Z. (2011). Influence of selected hydrophobic agents on some properties of autoclaving cellular concrete (ACC). *Construction and Building Materials, 25*(1), 282–287. https://doi.org/10.1016/j.conbuildmat.2010.06.028

Bonakdar, A., Babbitt, F., & Mobasher, B. (2013). Physical and mechanical characterization of fiber-reinforced aerated concrete (FRAC). *Cement and Concrete Composites, 38*, 82–91. https://doi.org/10.1016/j.cemconcomp.2013.03.006

Cai, L., Li, X., Liu, W., Ma, B., & Lv, Y. (2019). The slurry and physical-mechanical performance of autoclaved aerated concrete with high content solid wastes: Effect of grinding process. *Construction and Building Materials, 218*, 28–39. https://doi.org/10.1016/j.conbuildmat.2019.05.107

Campanale, M., Deganello, M., & Moro, L. (2013). Effect of moisture movement on tested thermal conductivity of moist aerated autoclaved concrete. *Transport in Porous Media, 98*(1), 125–146. https://doi.org/10.1007/s11242-013-0136-z

Campanale, M., & Moro, L. (2016). Thermal conductivity of moist autoclaved aerated concrete: Experimental comparison between heat flow method (HFM) and transient plane source technique (TPS). *Transport in Porous Media, 113*(2), 345–355. https://doi.org/10.1007/s11242-016-0697-8

Chen, G., Li, F., Jing, P., Geng, J., & Si, Z. (2021). Effect of pore structure on thermal conductivity and mechanical properties of autoclaved aerated concrete. *Materials, 14*(2), 339. https://doi.org/10.3390/ma14020339

Choo, H., Won, J., & Burns, S. E. (2021). Thermal conductivity of dry fly ashes with various carbon and biomass contents. *Waste Management, 135*, 122–129. https://doi.org/10.1016/j.wasman.2021.08.033

Cicek, T., & Tanrıverdi, M. (2007). Lime based steam autoclaved fly ash bricks. *Construction and Building Materials, 21*(6), 1295–1300. https://doi.org/10.1016/j.conbuildmat.2006.01.005

Collet, F., & Pretot, S. (2014). Thermal conductivity of hemp concretes: Variation with formulation, density and water content. *Construction and Building Materials, 65*, 612–619. https://doi.org/10.1016/j.conbuildmat.2014.05.039

Cong, X., Lu, S., Yao, Y., & Wang, Z. (2016). Fabrication and characterization of self-ignition coal gangue autoclaved aerated concrete. *Materials & Design, 97*, 155–162. https://doi.org/10.1016/j.matdes.2016.02.068

Dey, V., Bonakdar, A., & Mobasher, B. (2014). Low-velocity flexural impact response of fiber-reinforced aerated concrete. *Cement and Concrete Composites, 49*, 100–110. https://doi.org/10.1016/j.cemconcomp.2013.12.006

Dziekan, E., Laska, J., & Małolepszy, J. (2011). Influence of polymer superplasticizers on the properties of autoclaved aerated concrete.

Fouad, F. H., & Schoch, T. (2018). AAC in the USA—A second look. *Ce/papers, 2*(4), E1–E6. https://doi.org/10.1002/cepa.902

Hamad, A. J. (2014). Materials, production, properties and application of aerated lightweight concrete: Review. *International Journal of Materials Science and Engineering*. https://doi.org/10.12720/ijmse.2.2.152-157

Hauser, A., Eggenberger, U., & Mumenthaler, T. (1999). Fly ash from cellulose industry as secondary raw material in autoclaved aerated concrete. *Cement and Concrete Research, 29*(3), 297–302. https://doi.org/10.1016/s0008-8846(98)00207-5

Hoff, G. C. (1972). Porosity-strength considerations for cellular concrete. *Cement and Concrete Research, 2*(1), 91–100. https://doi.org/10.1016/0008-8846(72)90026-9

Holt, E., & Raivio, P. (2005). Use of gasification residues in aerated autoclaved concrete. *Cement and Concrete Research, 35*(4), 796–802. https://doi.org/10.1016/j.cemconres.2004.05.005

Hong, S., & Glasser, F. (2004). Phase relations in the $CaO–SiO_2–H_2O$ system to 200 °C at saturated steam pressure. *Cement and Concrete Research, 34*(9), 1529–1534. https://doi.org/10.1016/j.cemconres.2003.08.009

Hu, W., Neufeld, R. D., Vallejo, L. E., Kelly, C., & Latona, M. (1997). Strength properties of autoclaved cellular concrete with high volume fly ash. *Journal of Energy Engineering, 123*(2), 44–54. https://doi.org/10.1061/(asce)0733-9402(1997)123:2(44)

Huang, X., Ni, W., Cui, W., Wang, Z., & Zhu, L. (2012). Preparation of autoclaved aerated concrete using copper tailings and blast furnace slag. *Construction and Building Materials, 27*(1), 1–5. https://doi.org/10.1016/j.conbuildmat.2011.08.034

Hussin, M. W., Muthusamy, K., & Zakaria, F. (2010). Effect of mixing constituent toward engineering properties of POFA cement-based aerated concrete. *Journal of Materials in Civil Engineering, 22*(4), 287–295. https://doi.org/10.1061/(asce)0899-1561(2010)22:4(287)

Isu, N., Ishida, H., & Mitsuda, T. (1995). Influence of quartz particle size on the chemical and mechanical properties of autoclaved aerated concrete (I) tobermorite formation. *Cement and Concrete Research, 25*(2), 243–248. https://doi.org/10.1016/0008-8846(95)00003-8

Jerman, M., Keppert, M., Výborný, J., & Černý, R. (2013). Hygric, thermal and durability properties of autoclaved aerated concrete. *Construction and Building Materials, 41*, 352–359. https://doi.org/10.1016/j.conbuildmat.2012.12.036

Jiang, J., Cai, Q., Ma, B., Hu, Y., Qian, B., Ma, F., Shao, Z., Xu, Z., & Wang, L. (2021). Effect of ZSM-5 waste dosage on the properties of autoclaved aerated concrete. *Construction and Building Materials, 278*, 122114. https://doi.org/10.1016/j.conbuildmat.2020.122114

Jin, H., Yao, X., Fan, L., Xu, X., & Yu, Z. (2016). Experimental determination and fractal modeling of the effective thermal conductivity of autoclaved aerated concrete: Effects of moisture content. *International Journal of Heat and Mass Transfer, 92*, 589–602. https://doi.org/10.1016/j.ijheatmasstransfer.2015.08.103

Jo, B., Kim, C., Tae, G., & Park, J. (2007). Characteristics of cement mortar with nano-SiO_2 particles. *Construction and Building Materials, 21*(6), 1351–1355. https://doi.org/10.1016/j.conbuildmat.2005.12.020

Kalpana, M., & Mohith, S. (2020). Study on autoclaved aerated concrete: Review. *Materials Today: Proceedings, 22*, 894–896. https://doi.org/10.1016/j.matpr.2019.11.099

Karakurt, C., Kurama, H., & Topçu, İB. (2010). Utilization of natural zeolite in aerated concrete production. *Cement and Concrete Composites, 32*(1), 1–8. https://doi.org/10.1016/j.cemconcomp.2009.10.002

Kerienė, J., Kligys, M., Laukaitis, A., Yakovlev, G., Špokauskas, A., & Aleknevičius, M. (2013). The influence of multi-walled carbon nanotubes additive on properties of non-autoclaved and autoclaved aerated concretes.

Construction and Building Materials, 49, 527–535. https://doi.org/10.1016/j.conbuildmat.2013.08.044

Kikuma, J., Tsunashima, M., Ishikawa, T., Matsuno, S., Ogawa, A., Matsui, K., & Sato, M. (2011). Effects of quartz particle size and water-to-solid ratio on hydrothermal synthesis of tobermorite studied by in-situ time-resolved X-ray diffraction. *Journal of Solid-State Chemistry, 184*(8), 2066–2074. https://doi.org/10.1016/j.jssc.2011.05.061

Klimesch, D. S., Ray, A., & Sloane, B. (1996). Autoclaved cement-quartz pastes: The effects on chemical and physical properties when using ground quartz with different surface areas part I: Quartz of wide particle size distribution. *Cement and Concrete Research, 26*(9), 1399–1408. https://doi.org/10.1016/0008-8846(96)00117-2

Kreft, O., Hausmann, J., Hubálková, J., Aneziris, C. G., Straube, B., & Schoch, T. (2011, September). Pore size distribution effects on the thermal conductivity of light weight autoclaved aerated concrete. In *5th International conference on autoclaved aerated concrete, Bydgoscsz, Poland* (pp. 257–264).

Kumar, R. (2020). Modified mix design and statistical modelling of lightweight concrete with high volume micro fines waste additive via the Box–Behnken design approach. *Cement and Concrete Composites, 113*, 103706. https://doi.org/10.1016/j.cemconcomp.2020.103706

Kumar, R. (2021). Effects of high volume dolomite sludge on the properties of eco-efficient lightweight concrete: Microstructure, statistical modeling, multi-attribute optimization through derringer's desirability function, and life cycle assessment. *Journal of Cleaner Production, 307*, 127107. https://doi.org/10.1016/j.jclepro.2021.127107

Kumar, R., & Lakhani, R. (2021). Development of lightweight aggregate concrete with optimum thermal transmittance for opaque wall assembly in composite climates. Abstracts of International Conferences & Meetings. https://doi.org/10.5281/zenodo.5051936

Kumar, R., Lakhani, R., & Kumar, A. (2021a). Physico-mechanical and thermal properties of lightweight structural concrete with light expanded clay aggregate for energy-efficient buildings. *Lecture Notes in Civil Engineering*. https://doi.org/10.1007/978-981-16-6557-8_14

Kumar, R., Lakhani, R., & Tomar, P. (2018). A simple novel mix design method and properties assessment of foamed concretes with limestone slurry waste. *Journal of Cleaner Production, 171*, 1650–1663. https://doi.org/10.1016/j.jclepro.2017.10.073

Kumar, R., & Srivastava, A. (2022). Influence of lightweight aggregates and supplementary cementitious materials on the properties of lightweight aggregate concretes. *Iranian Journal of Science and Technology, Transactions of Civil Engineering*. https://doi.org/10.1007/s40996-022-00935-5

Kumar, R., Srivastava, A., & Lakhani, R. (2021b). Industrial wastes-cum-strength enhancing additives incorporated lightweight aggregate concrete (LWAC) for energy efficient building: A comprehensive review. *Sustainability, 14*(1), 331. https://doi.org/10.3390/su14010331

Kunchariyakun, K., Asavapisit, S., & Sinyoung, S. (2018). Influence of partial sand replacement by black rice husk ash and bagasse ash on properties of autoclaved aerated concrete under different temperatures and times. *Construction and Building Materials, 173*, 220–227. https://doi.org/10.1016/j.conbuildmat.2018.04.043

Kunchariyakun, K., Asavapisit, S., & Sombatsompop, K. (2015). Properties of autoclaved aerated concrete incorporating rice husk ash as partial replacement for fine aggregate. *Cement and Concrete Composites, 55*, 11–16. https://doi.org/10.1016/j.cemconcomp.2014.07.021

Kurama, H., Topçu, İ, & Karakurt, C. (2009). Properties of the autoclaved aerated concrete produced from coal bottom ash. *Journal of Materials Processing Technology, 209*(2), 767–773. https://doi.org/10.1016/j.jmatprotec.2008.02.044

Lakhani, R., & Kumar, R. (2015). Effective utilization of limestone slurry waste as partial replacement of sand for non-structural cellular foamed concrete blocks. In *International conference on sustainable structural concrete. RILEM*.

Lam, N. T., Asamoto, S., & Matsui, K. (2018). Microstructure and shrinkage behavior of autoclaved aerated con-crete(aac)-comparison of Vietnamese and Japanese aacs-. *Journal of Advanced Concrete Technology, 16*(8), 333–342. https://doi.org/10.3151/jact.16.333

Laukaitis, A., Keriene, J., Kligys, M., Mikulskis, D., & Lekunaite, L. (2010). Influence of amorphous nanodispersive SiO_2 additive on structure formation

Abhilasha *et al. Int J Concr Struct Mater* (2023) 17:6

Page 21 of 22

and properties of autoclaved aerated concrete. *Materials Science, 16*(3), 257–263.

Laukaitis, A., Kerienė, J., Mikulskis, D., Sinica, M., & Sezemanas, G. (2009). Influence of fibrous additives on properties of aerated autoclaved concrete forming mixtures and strength characteristics of products. *Construction and Building Materials, 23*(9), 3034–3042. https://doi.org/10.1016/j.conbuildmat.2009.04.007

Lekūnaitė, L., Laukaitis, A., Kligys, M., & Mikulskis, D. (2012). Investigations of forming mixture parameters of autoclaved aerated concrete with nanoadditives. *Materials Science*. https://doi.org/10.5755/j01.ms.18.3.2441

Ma, B., Cai, L., Li, X., & Jian, S. (2016). Utilization of iron tailings as substitute in autoclaved aerated concrete: Physico-mechanical and microstructure of hydration products. *Journal of Cleaner Production, 127*, 162–171. https://doi.org/10.1016/j.jclepro.2016.03.172

Mehta, P. K., & Monteiro, P. J. (2013). *Concrete microstructure, properties and materials* (4th ed.). McGraw-Hill Education.

Mostafa, N. (2005). Influence of air-cooled slag on physicochemical properties of autoclaved aerated concrete. *Cement and Concrete Research, 35*(7), 1349–1357. https://doi.org/10.1016/j.cemconres.2004.10.011

Mostafa, N. Y. (1995). Factors effecting the hydrothermal reactions in $CaO-SiO_2-H_2O$ system (Doctoral dissertation, MSc thesis, Suez Canal University).

Mostafa, N., El-Hemaly, S., Al-Wakeel, E., El-Korashy, S., & Brown, P. (2001). Activity of silica fume and dealuminated kaolin at different temperatures. *Cement and Concrete Research, 31*(6), 905–911. https://doi.org/10.1016/s0008-8846(01)00489-6

Munir, M. J., Kazmi, S. M., Wu, Y., Hanif, A., & Khan, M. U. (2018). Thermally efficient fired clay bricks incorporating waste marble sludge: An industrial-scale study. *Journal of Cleaner Production, 174*, 1122–1135. https://doi.org/10.1016/j.jclepro.2017.11.060

Narayanan, N., & Ramamurthy, K. (2000). Structure and properties of aerated concrete: A review. *Cement and Concrete Composites, 22*(5), 321–329. https://doi.org/10.1016/s0958-9465(00)00016-0

Nielsen, A. (1983). Shrinkage and creep-deformation parameters of aerated, autoclaved concrete. *Proceedings autoclaved aerated concrete, moisture and properties* (pp. 189–205). Elsevier.

Papatzani, S., Paine, K., & Calabria-Holley, J. (2015). A comprehensive review of the models on the nanostructure of calcium silicate hydrates. *Construction and Building Materials, 74*, 219–234. https://doi.org/10.1016/j.conbuildmat.2014.10.029

Pehlivanlı, Z. O., Uzun, İ, & Demir, İ. (2015). Mechanical and microstructural features of autoclaved aerated concrete reinforced with autoclaved polypropylene, carbon, Basalt and glass fiber. *Construction and Building Materials, 96*, 428–433. https://doi.org/10.1016/j.conbuildmat.2015.08.104

Pehlivanlı, Z. O., Uzun, İ, Yücel, Z. P., & Demir, İ. (2016). The effect of different fiber reinforcement on the thermal and mechanical properties of autoclaved aerated concrete. *Construction and Building Materials, 112*, 325–330. https://doi.org/10.1016/j.conbuildmat.2016.02.223

Pellenq, R. J., Kushima, A., Shahsavari, R., Van Vliet, K. J., Buehler, M. J., Yip, S., & Ulm, F. (2009). A realistic molecular model of cement hydrates. *Proceedings of the National Academy of Sciences, 106*(38), 16102–16107. https://doi.org/10.1073/pnas.0902180106

Perumalsamy, N., Sankar, A., Preethi, R. C., Rizwan, P. S., Sheela, S., Sekar, C., & Arumaikkani, G. (2018). Effective review on utilization of wastes in aerated cellular concrete. *Journal of Chemical and Pharmaceutical Research, 10*(3), 127–141.

Petrov, I., & Schlegel, E. (1994). Application of automatic image analysis for the investigation of autoclaved aerated concrete structure. *Cement and Concrete Research, 24*(5), 830–840. https://doi.org/10.1016/0008-8846(94)90003-5

Prim, P., & Wittmann, F. H. (1983). *Structure and water absorption of aerated concrete: Autoclaved aerated concrete, moisture and properties*. Elsevier.

Qu, X., & Zhao, X. (2017). Previous and present investigations on the components, microstructure and main properties of autoclaved aerated concrete—A review. *Construction and Building Materials, 135*, 505–516. https://doi.org/10.1016/j.conbuildmat.2016.12.208

Rahman, R., Fazlizan, A., Asim, N., & Thongtha, A. (2020). Utilization of waste material for aerated autoclaved concrete production: A preliminary review. *IOP Conference Series: Earth and Environmental Science, 463*(1), 012035. https://doi.org/10.1088/1755-1315/463/1/012035

Rahman, R., Fazlizan, A., Asim, N., & Thongtha, A. (2021). A review on the utilization of waste material for autoclaved aerated concrete production. *Journal of Renewable Materials, 9*(1), 61–72. https://doi.org/10.32604/jrm.2021.013296

Ramamurthy, K., & Narayanan, N. (2000). Influence of composition and curing on drying shrinkage of aerated concrete. *Materials and Structures, 33*(4), 243–250. https://doi.org/10.1007/bf02479334

Różycka, A., & Pichór, W. (2016). Effect of perlite waste addition on the properties of autoclaved aerated concrete. *Construction and Building Materials, 120*, 65–71. https://doi.org/10.1016/j.conbuildmat.2016.05.019

Sato, H., & Grutzeck, M. (1991). Effect of starting materials on the synthesis of Tobermorite. *MRS Proceedings*. https://doi.org/10.1557/proc-245-235

Schober, G. (2005). The most important aspects of microstructure influencing strength of AAC. *AAC, Taylor*.

Schober, G. (2011, September). Porosity in autoclaved aerated concrete (AAC): A review on pore structure, types of porosity, measurement methods and effects of porosity on properties. In *5th international conference on autoclaved aerated concrete* (No. 39–43, pp. 351–359). Bydgoscsz Poland.

Serhat Baspinar, M., Demir, I., Kahraman, E., & Gorhan, G. (2013). Utilization potential of fly ash together with silica fume in autoclaved aerated concrete production. *KSCE Journal of Civil Engineering, 18*(1), 47–52. https://doi.org/10.1007/s12205-014-0392-7

Sinica, M., Sezeman, G. A., Mikulskis, D., Kligys, M., & Česnauskas, V. (2014). Impact of complex additive consisting of continuous Basalt fibres and SiO_2 microdust on strength and heat resistance properties of autoclaved aerated concrete. *Construction and Building Materials, 50*, 718–726. https://doi.org/10.1016/j.conbuildmat.2013.10.027

Song, Y., Li, B., Yang, E., Liu, Y., & Ding, T. (2015). Feasibility study on utilization of municipal solid waste incineration bottom ash as aerating agent for the production of autoclaved aerated concrete. *Cement and Concrete Composites, 56*, 51–58. https://doi.org/10.1016/j.cemconcomp.2014.11.006

Subash, M. C. G., Satyannarayana, V. S. V., & Srinivas, J. (2016). Aerated autoclaved concrete (AAC) blocks: A revolution building material in construction industry. *International Journal of Science Technology and Management, 5*(1), 167–174.

Tada, S. (1986). Material design of aerated concrete—An optimum performance design. *Materials and Structures, 19*(1), 21–26. https://doi.org/10.1007/bf02472306

Tanyildizi, H. (2008). Effect of temperature, carbon fibers, and silica fume on the mechanical properties of lightweight concretes. *New Carbon Materials, 23*(4), 339–344. https://doi.org/10.1016/s1872-5805(09)60005-6

Taylor, H. F. (1997). *Cement chemistry* (Vol. 2, p. 459). Thomas Telford.

Thongtha, A., Maneewan, S., Punlek, C., & Ungkoon, Y. (2014). Investigation of the compressive strength, time lags and decrement factors of AAC-lightweight concrete containing sugar sediment waste. *Energy and Buildings, 84*, 516–525. https://doi.org/10.1016/j.enbuild.2014.08.026

Topçu, İB., & Uygunoğlu, T. (2007). Properties of autoclaved lightweight aggregate concrete. *Building and Environment, 42*(12), 4108–4116. https://doi.org/10.1016/j.buildenv.2006.11.024

Walczak, P., Małolepszy, J., Reben, M., Szymański, P., & Rzepa, K. (2015a). Utilization of waste glass in Autoclaved aerated concrete. *Procedia Engineering, 122*, 302–309. https://doi.org/10.1016/j.proeng.2015.10.040

Walczak, P., Szymański, P., & Różycka, A. (2015b). Autoclaved aerated concrete based on fly ash in density 350 kg/m^3 as an environmentally friendly material for energy—Efficient constructions. *Procedia Engineering, 122*, 39–46. https://doi.org/10.1016/j.proeng.2015.10.005

Wan, H., Hu, Y., Liu, G., & Qu, Y. (2018). Study on the structure and properties of autoclaved aerated concrete produced with the stone-sawing mud. *Construction and Building Materials, 184*, 20–26. https://doi.org/10.1016/j.conbuildmat.2018.06.214

Wang, C., Ni, W., Zhang, S., Wang, S., Gai, G., & Wang, W. (2016). Preparation and properties of autoclaved aerated concrete using coal gangue and iron ore tailings. *Construction and Building Materials, 104*, 109–115. https://doi.org/10.1016/j.conbuildmat.2015.12.041

Wongkeo, W., & Chaipanich, A. (2010). Compressive strength, microstructure and thermal analysis of autoclaved and air cured structural lightweight concrete made with coal bottom ash and silica fume. *Materials Science and Engineering: A, 527*(16–17), 3676–3684. https://doi.org/10.1016/j.msea.2010.01.089

Wongkeo, W., Thongsanitgarn, P., Pimraksa, K., & Chaipanich, A. (2012). Compressive strength, flexural strength and thermal conductivity of

autoclaved concrete block made using bottom ash as cement replacement materials. *Materials & Design, 35*, 434–439. https://doi.org/10.1016/j.matdes.2011.08.046

Yaman, N., & Abd Rashid, A. F. (2021). The potential of carbon footprint reduction of a mid-rise residential building in Sarawak. *Built Environment Journal, 18*(1), 1. https://doi.org/10.24191/bej.v18i1.12195

Yang, J., Shi, Y., Yang, X., Liang, M., Li, Y., Li, Y., & Ye, N. (2013). Durability of autoclaved construction materials of sewage sludge–cement–fly ash–furnace slag. *Construction and Building Materials, 48*, 398–405. https://doi.org/10.1016/j.conbuildmat.2013.07.018

Zafar, M. S., Javed, U., Khushnood, R. A., Nawaz, A., & Zafar, T. (2020). Sustainable incorporation of waste granite dust as partial replacement of sand in autoclave aerated concrete. *Construction and Building Materials, 250*, 118878. https://doi.org/10.1016/j.conbuildmat.2020.118878

Zeminian, N., Guarino, G., & Xu, Q. (2018). Chemical admixtures for the optimization of the AAC production. *Ce/papers, 2*(4), 235–240. https://doi.org/10.1002/cepa.828

Zhao, Y., Zhang, Y., Chen, T., Chen, Y., & Bao, S. (2012). Preparation of high strength autoclaved bricks from hematite tailings. *Construction and Building Materials, 28*(1), 450–455. https://doi.org/10.1016/j.conbuildmat.2011.08.078

Zollo, R. F. (1997). Fiber-reinforced concrete: An overview after 30 years of development. *Cement and Concrete Composites, 19*(2), 107–122. https://doi.org/10.1016/s0958-9465(96)00046-7

Publisher's Note